Dissertation
submitted to the
Combined Faculties for the Natural Sciences and for Mathematics
of the Ruperto-Carola University of Heidelberg, Germany
for the degree of
Doctor of Natural Sciences

The necessity of *Tb*CNOT10 in the process of mRNA turnover

presented by
Diplom-Biologe Valentin Lutz Fabian Färber
born in Ostfildern-Ruit, Germany
Oral-examination: 28th September 2012

Referees:

1. Prof. Dr. Christine Clayton
   Zentrum für Molekulare Biologie der Universität Heidelberg (ZMBH)
   Im Neuenheimer Feld 282
   69120 Heidelberg

2. Dr. Georg Stoecklin
   Deutsches Krebsforschungszentrum (DKFZ)
   Im Neuenheimer Feld 282
   69120 Heidelberg

For Cristiana

Acknowledgement

Ich möchte mich zuerst bei Prof. Christine Clayton bedanken, dass Sie mich in Ihre Arbeitsgruppe aufgenommen und mir die Möglichkeit geben hat, dieses spannende Thema zu bearbeiten. Mein Dank gilt Ihr auch für die vielen Diskussionen und Ratschläge, während meiner Doktorarbeit. Hervorzuheben ist auch Ihre Bereitschaft meine Doktorarbeit an einem sonnigen Sonntag durchzuschauen.

Ich möchte mich auch bei Dr. Georg Stöcklin bedanken, dass er das Zweitgutachten übernommen hat und für seine vielen guten Ratschläge, während der TAC Meetings.

Vielen Dank auch an Prof. Luise Krauth-Siegel für die guten Diskussionen während der TAC Meetings und den schönen Seminaren.

Mein Dank gilt auch allen alten sowie jetzigen Mitgliedern der Arbeitsgruppe Clayton für die schönen Movie Nights, BBQs und sonstigen Aktivitäten. Es hat zu einer hervorragenden Atmosphäre beigetragen, die ich immer in guter Erinnerung behalten werde. Ein besonderer Dank geht auch an Doro und Diana, für das Korrektur lesen meiner Arbeit.

Zum Schluss möchte ich mich auch bei meiner Familie bedanken, die mich immer unterstützt und motiviert hat.

I. Table of Contents

I. Zusammenfassung

Messenger RNA Degradierung startet mit Deadenylierung durch den CCR4-CAF1-NOT Komplex und darauf folgt entweder 5' -> 3' oder 3' -> 5' mRNA-Verdau. In dem protozoen Parasiten *T. brucei* wird die Genexpression hauptsächlich auf der Ebene des mRNA-Verdaus kontrolliert. In dem Parasitengenom existiert CCR4 nicht und daher wird der Komplex hier CAF1-NOT genannt. Wie in anderen Eukaryoten ist der Komplex auf dem Gerüstprotein NOT1 aufgebaut, an den sich die restlichen Untereinheiten CAF1, CAF40, NOT2, NOT3/5, DHH1 und ein CNOT10-ähnliches Protein anlagern. Obwohl es bekannt ist, dass CAF1 die katalytische Untereinheit ist, sind die Funktion der anderen Untereinheiten unbekannt.

Während meiner Doktorarbeit habe ich mich auf die Charakterisierung von *Tb*CNOT10 konzentriert; kodiert durch den Genlokus *Tb*927.10.8720. In Trypanosomen ist *Tb*CNOT10 ungefähr 20 kDa kleiner als sein menschlicher Gegenpart und hat nur eine Sequenzidentität von rund 22 %. Ich konnte zeigen, dass *Tb*CNOT10 ein stabiler Bestandteil des Komplexes ist und direkt mit CAF1 und NOT1 interagiert. Reduzierung von *Tb*CNOT10 führte zu einen Vermehrungsdefekt des Parasiten in beiden Lebensstadien und interessanterweise, destabilisierte den CAF1-NOT Komplex. Als ich den RNAi-Effekt von *Tb*CNOT10 weiter studierte, konnte ich sehen, dass seine Reduzierung zu einer Verringerung der NOT1 Menge führte und dass sich CAF1 vom Komplex ablöste. Durch die Verwendung von RNA-Sequenzierung, um die transkriptomweite mRNA-Degradation zu messen, konnte ich in *Tb*CNOT10 sowie in CAF1 armen Zellen beobachten, dass die mRNA-Degradierung stoppte. Einen ähnlichen Effekt konnte ich für RRP45 RNAi erkennen, während ein Knockdown von PAN2 das Transkriptom nicht beeinträchtigte. *In vivo* Bindungsassays mit CAF1 und einem mRNA-Reporter in *Tb*CNOT10 armen Zellen zeigte, dass die CAF1 Aktivität vom Komplex unabhängig ist. Studien in Säugetierzellen zeigten, dass menschliches CNOT10 nicht für die Assoziation von CAF1a mit NOT1 benötigt wird. Meine Ergebnisse lassen vermuten, dass *Tb*CNOT10 in Trypanosomen für die Bindung von CAF1 mit dem Komplex benötigt wird und dass CAF1 alleine unfähig ist, Poly(A)-binding protein (PABP) geschützte mRNAs zu deadenylieren.

II. Summary

mRNA degradation starts with deadenylation by the CCR4-CAF1-NOT complex, which is followed by either 5'->3' or 3'->5' digestion. In the protozoan parasite *T. brucei*, gene expression is controlled mainly at the level of mRNA degradation. In this parasite, CCR4 is absent and hence the complex is called CAF1-NOT. As in other eukaryotes, the complex is built on the scaffold protein NOT1, to which are attached the remaining subunits: CAF1, CAF40, NOT2, NOT3/5, TbDHH1 and a CNOT10-like protein. Although it is clear that CAF1 is the catalytic subunit, the functions of the other subunits are unknown.

During my PhD, I focused on the characterization of *Tb*CNOT10, encoded by the gene locus Tb927.10.8720. *Tb*CNOT10 is around 20 kDa smaller than its human counterpart and has a sequence identity of only about 22 %. I could show that *Tb*CNOT10 is a stable component of the complex and interacts directly with CAF1 and NOT1. Depletion of *Tb*CNOT10 led to a proliferation defect in both life stages of the parasite and, more interestingly, destabilized the CAF1-NOT complex. When I further investigated the effect of *Tb*CNOT10 RNAi, I could see that its depletion led to a decrease in NOT1 abundance and detachment of CAF1 from the complex. Using RNA sequencing to measure transcriptome-wide RNA degradation, I observed that mRNA degradation came to a halt in *Tb*CNOT10- and CAF1-depleted cells. A similar effect could be observed for RRP45 RNAi, whereas a knock down of PAN2 did not affect the transcriptome. Tethering assays *in vivo* with CAF1 and an mRNA reporter in *Tb*CNOT10-depleted cells showed that the activity of CAF1 is complex-independent. Studies in mammalian cells demonstrated that human CNOT10 is not required for the association of CAF1a with NOT1. Finally, my results suggest that in trypanosomes, CNOT10 is needed for the attachment of CAF1 with the complex and that CAF1 alone is unable to deadenylate Poly(A)-binding protein (PABP) protected mRNAs.

III. Introduction

In this study, I use the model organism *Trypanosoma brucei* in order to investigate the role of the putative CNOT10 homologue in the process of mRNA turnover.

III.1. The role of mRNA degradation

Messenger RNA (mRNA) degradation is important in the control of gene expression. It regulates the level of mRNA transcripts and hence helps to define the amounts of translated proteins. If mRNA degradation is deregulated, it can lead to a variety of different diseases like cancer (1-4), chronic inflammation (e.g. arthritis) (3-5), neurodegenerative disease (6).

III.2. Life and death of an mRNA

In all organisms, messenger RNAs (mRNAs) are the carriers of genetic information from the nucleus into the cytoplasm. Figure 1 shows an overview of the different pathways an mRNA can follow. Transcription, processing and export determine the steady-state level of mRNAs. However, another major determiner of the amount of transcripts in the cell is mRNA turnover.

Transcriptome-wide studies measuring mRNA turnover through the use of microarrays or RNAseq, showed major differences in mRNA half-lives between analysed organisms. In prokaryotes for instance, the median half-life was 5 min (7), whereas for the simple eukaryotes *Trypanosoma brucei* (*T. brucei*) and yeast, a median half-life of respectively 13 min and 21 min was obtained (8-10). Longer median half-lives lasting from 4 to 10 hours were yielded for different types of mammalian cells (11-13), and Arabidopsis also showed a median half-life of 3.8 h (14). The common point between all these studies was that related groups of mRNAs exhibited similar mRNA half-lives.

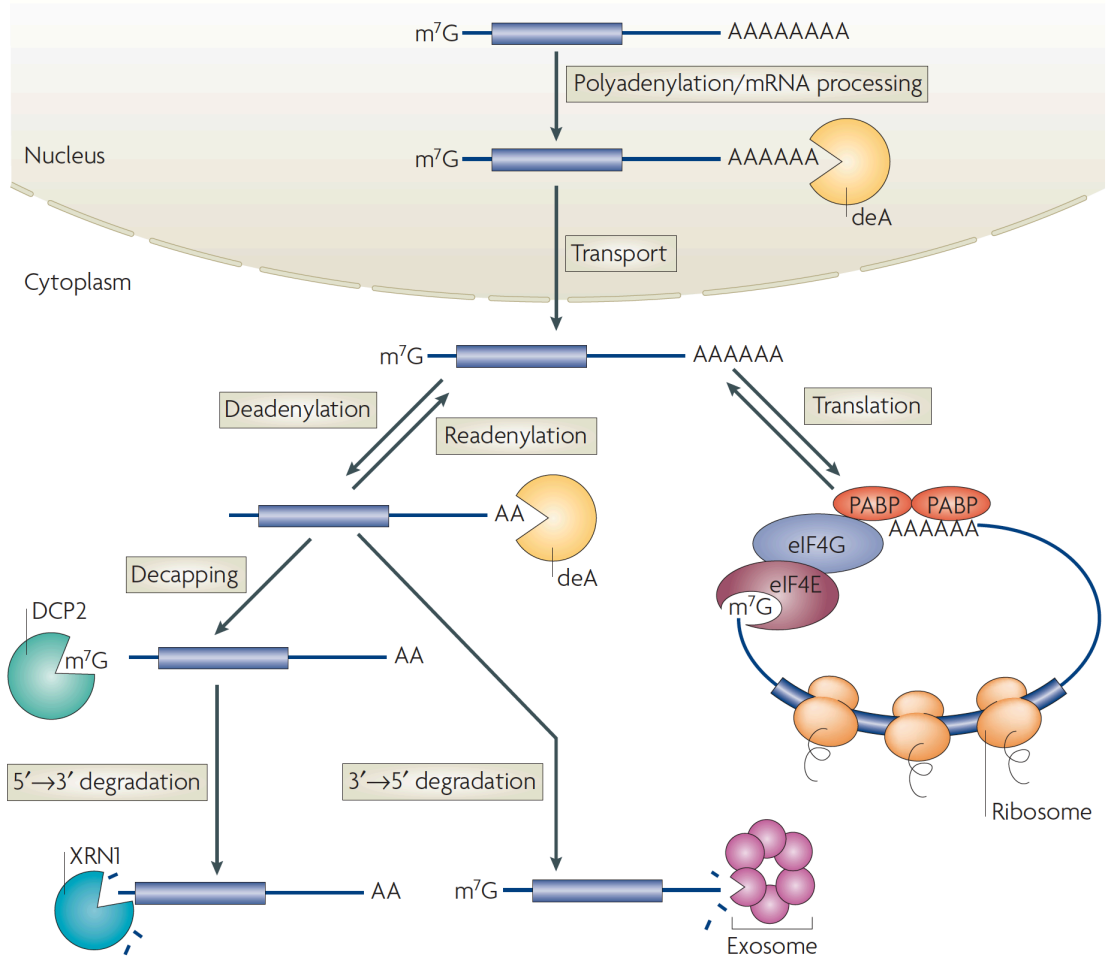

Figure 1 Fate of an mRNA in eukaryotes

An mRNA can follow several different pathways once it is transcribed. The first step is processing and polyadenylation, which is then followed by the transport of the mRNA from the nucleus to the cytoplasm. Here the mRNA is either translated or targeted for degradation. The first step of degradation is the removal of the poly(A) tail which leads to decapping. Now mRNAs can be degraded by XRN1, or the exosome (Taken from 15).

In the 3'UTR of mRNAs, stabilising but also destabilising elements have evolved in order to control the half-life of an mRNA. The 5' end of every mRNA is protected by a cap structure along with the cap-binding protein eIF4E that prevents mRNA degradation by 5' exoribonucleases. There is also a poly(A) tail with protective poly(A) binding proteins at the 3' end to ensure a certain protection from 3' exoribonucleases. To further defend the coding sequence (CDS) from exonucleolytic attacks and increase the rate of its translation, mRNAs can form a loop structure by the interaction of eIF4E with PABP through eIF4G (16-18). For proper gene expression, it is also essential

that no longer necessary mRNAs can easily be targeted to mRNA degradation. Therefore, *cis*-acting elements have evolved in the 3'untranslated region (UTR) of mRNAs. One of the most prominent members is the AU-rich element (ARE), which promotes rapid degradation. This element can be found in many mRNAs encoding for proteins that are important for growth or for the response to inflammations (19, 20). Besides destabilising elements, there are also elements that can lead to the stabilisation of mRNAs (e.g. nucleolin-binding element for beta-globin stabilisation) (21).

It is widely accepted that deadenylation is the initial step of mRNA decay (22, 23). The current model suggests that in yeast and mammalian cells the PAN2-PAN3 complex is responsible for the initial shortening of the poly(A) tail and is followed by the major deadenylation complex CCR4-CAF1-NOT (23-26). The CCR4-CAF1-NOT complex deadenylates the poly(A) tail under a certain threshold (10 nt), which is below the minimum sequence length for PABP binding (12 – 14 nt) and hence leads to dissociation of PABP (27-29). By doing so, the interaction between the 3' and 5' end of the mRNA becomes disrupted, which leads to a cleavage of the protective cap structure by DCP2 along with DCP1 (30, 31). In human and *Drosophila,* it was shown that Pat1 links deadenylation and decapping by interacting simultaneously with the decapping complex DCP1-DCP2 and the CCR4-CAF1-NOT complex (32, 33). It also interacts with the Lsm1-7 proteins, Edc1-3, Hedls and the 5′-3′ exoribonuclease XRN1 (33, 34). However, some mRNAs are decapped in a deadenylation-independent manner, as for instance mRNAs with a premature termination codon (35) or histone mRNAs from mammalian cells lacking a poly (A) tail (36). The unprotected mRNA can be degraded either from the 5' end by XRN1 or by the exosome and the decapping scavenger in the 3' direction (22). It was recently shown that degradation by XRN1 could also occur co-translationally, allowing ribosomes to finish their round of translation (37). The upcoming sub-chapters will focus on the above-mentioned enzymes and the way they function in the process of mRNA turnover.

III.3. Deadenylation complexes

As stated previously, mRNA degradation starts with deadenylation. In eukaryotes, three deadenylase complexes have been described: the poly(A)-specific ribonuclease (PARN) that forms homodimers, PAN2-PAN3 and the CCR4-CAF1-NOT complex, also called CAF1-NOT, due to the absence of CCR4 (38, 39).

III.3.1. The poly(A)-specific ribonuclease PARN

The poly(A)-specific ribonuclease (PARN) belongs to the group of DEDD exonucleases. It was localised in the nucleus (cajal body and nucleoli) and in discrete foci in the cytoplasm in mammalian cells and plants (40-42). PARN differs from all other deadenylases in the fact that it is stimulated by its interaction with the cap structure of mRNAs (43, 44). The nuclease activity was confirmed in mammalian *in vitro* decay systems, with mRNAs possessing or lacking a cap structure (45-47). So far, it was shown that it functions in the maturation of *Xenopus* as well as mouse oocytes and plant embryogenesis (42, 48, 49). For instance, in *Xenopus* oocytes, it is responsible for the deadenylation of dormant mRNAs (e.g. cyclin B1) without inducing mRNA degradation. During maturation, PARN activity is inhibited and dormant mRNAs are polyadenylated by Gld-2, a poly(A) polymerase, in order to be translated (50). Additionally, PARN is essential for a proper stress response in Arabidopsis (51, 52). In mammalian cells, PARN could also be implicated in nonsense-mediated decay (53), decay of mRNAs containing AU-rich elements (41) and processing of snoRNA and scaRNA (40).

III.3.2. PAN2-PAN3 complex

The PAN2-PAN3 complex consists of the deadenylase PAN2 and its auxiliary protein PAN3. Like PARN, PAN2 belongs to the DEDD exonucleases. PAN3 interacts via its C-terminal part with PAN2 and with PABP through a PAM2 motif in its N-terminal part (54-56). The PAN2-PAN3 complex is stimulated by PABP (54, 57). Both in yeast and in trypanosomes,

the complex is located in the nucleus and cytoplasm (25, 26, 58), whereas in human cell lines, it could only be detected in the cytoplasm (54).

Most of the studies to characterise the PAN2-PAN3 complex were done in yeast. Here it was shown that a deletion of both proteins had no effect on the viability of *S. cerevisiae* (59, 60). However, longer poly(A) tails were observed upon deletion of PAN2 and PAN3. In the nucleus, the PAN2-PAN3 complex trims newly transcribed mRNAs to a specific length (25), whereas in the cytoplasm it is involved in the initial shortening of the poly(A) tail (25, 26). The implication of the PAN2-PAN3 complex with the initiation of deadenylation was also seen in mammalian cells (24). In *Drosophila* Schneider cells, the roles of PAN2 and CAF1 were studied in knockdown mutants, using a pulse chase approach. mRNA deadenylation of endogenous *hsp70* was studied after heat shock. A knockdown of PAN2 alone had no effect, whereas knocking down CAF1 led to an inhibition of *hsp70* deadenylation. This effect was increased when both were knocked down (61). In mammalian cells, the PAN2-PAN3 complex was found in P bodies and it was shown that PAN3 could enhance the localisation of the deadenylases PAN2, CCR4 and CAF1 (62). Using coimunoprecipitation and *in vitro* pull-down assays, human GW182 proteins were found to recruit PAN2-PAN3 through direct interaction with PAN3 (63).

III.3.3. CCR4-CAF1-NOT complex

The CCR4-CAF1-NOT complex, also known as the CAF1-NOT complex, is considered to be the major deadenylation complex in eukaryotes. Beside its role in deadenylation, it has also been implicated in the regulation of transcription, translation repression, the DNA damage response, mRNA export and nuclear surveillance (64).

In yeast, the complex consists of nine core subunits, Ccr4p, CAF1p, Caf40p, CAF130p and Not 1-5p, which can alternatively form two distinguishable subcomplexes of 1 and 2 MDa (65, 66). The smaller complex consists of Not2-5p and the bigger of Not1p, Ccr4p, CAF1p, Caf40p and CAF130p. Figure 2 shows a comparison of the CCR4-CAF1-NOT complex in yeast and the CAF1-NOT complex from trypanosomes. The structure and

composition of the NOT complex are based on glycerol gradient centrifugation studies and pulldown experiments. As a result, the illustrations are merely estimations and probably do not reflect reality but nevertheless help to understand the functions of the complex.

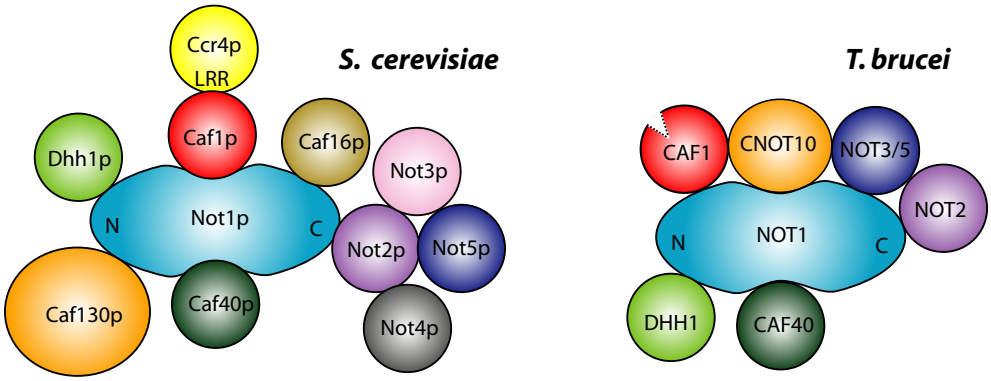

Figure 2 Comparison of the Ccr4-CAF1-Not complex in yeast and the CAF1-NOT complex of *Trypanosoma brucei*

The figure shows a simplified illustration of the Ccr4-Caf1-Not complex in yeast and the CAF1-NOT complex in *Trypanosoma brucei* in which homologous subunits are shown in the same colour. Because CNOT10 and CAF130p are potential homologues, both are shown in orange. NOT1 is the major scaffold to which the remaining subunits attach themselves. CCR4 and CAF1 are deadenylases of the complexes though Ccr4 is absent from the genome of trypanosomes. CAF16p and Not4p also do not have any obvious orthologues in the genome of *T. brucei*. DHH1 is a helicase and Not4p is an E3 ligase. The functions of the other subunits are unclear. (Figure was taken from Prof. CE Clayton and modified)

In contrast to the core complex from yeast, the human, *Drosophila* and trypanosome core complexes lack Not4 and have a single protein (NOT3/5) that is similar to the yeast subunits Not3p and Not5p (38, 67-69). In humans, two additional subunits have been identified: TAB182 and C2ORF29 (67). The knockdown of CAF1 and CCR4 along with subsequent deadenylation experiments permitted to identify CAF1 as the major deadenylase in eukaryotes, except for yeast where it is CCR4 (38, 64, 70-72). The human genome contains two homologues of CAF1 (also known as CNOT7 and 8 or CAF1a and b) and CCR4 (CNOT6 and 6L) and these account for four different variants of the CCR4-CAF1-NOT complex (67, 73). All complexes are built on the major scaffold Not1p that acts as a platform not only for the

remaining CCR4-CAF1-NOT core subunits, but also for specific mRNA degradation factors. For instance, human NOT1 is recruited to mRNAs containing AU-rich elements by Tis11 proteins (64, 74) and/or GW182/TNRC6, required for microRNA-induced mRNA decay (63, 75), which triggers their degradation in both cases. Due to its role as a scaffold, depletion of NOT1 in human and yeast led to the disruption of the complex and subsequently to a halt of mRNA deadenylation (76, 77). The functions of the other subunits Not2-5, Caf40 and CAF130/CNOT10 are unclear. Immunoprecipitation and gel filtration analyses with Not2p mutants in yeast led to the observation that Not2-5p proteins were not able to associate with the complex (78). In a further study in yeast, Caf40p was TAP-tagged and non-essential subunits of the complex were simultaneously knocked out. The knockout of Not2p resulted in the dissociation of CAF130p, Not4p and Not5p from the remaining Caf40p complex (77). In Not2 depleted mammalian cells the same observation could be made in gel filtration experiments (79). In yeast, Not3 is up to 44% identical to Not5, but in genome-wide expression studies using microarrays, Not3p and Not5p knockout mutants exhibit a specific gene expression pattern, indicating that they have distinct functions (77). More information is available about Not4. The human homologue of Not4p, CNOT4, was identified as a RING E3 ligase and NMR spectroscopy revealed the structure for the C_4C_4 RING (80). In the same study, the ubiquitin ligase activity could be verified *in vitro*. In yeast, it was shown that Not4p is involved in degrading aberrant polypeptides that lack a stop codon (80, 81). Not4p is a stable member of the CCR4-CAF1-NOT complex in yeast, but not in human and *Drosophila* (67, 68). In trypanosomes, NOT4 is absent from the genome (38). A crystal structure is available for Rcd-1, the human homologue of Caf40. It was found that Rcd-1 can dimerize and is able to bind ssDNA (82). CAF130p seems to be dispensable in yeast, since a CAF130p knockout did not influence growth and had also no effect on the transcriptome (77). It was shown that CAF130p interacts with the N- and C-terminus of Not1, and that it is not important for the stability of the complex (77, 83). Finally, very little is known about CNOT10. In order to figure out its role, CNOT10 was TAP-tagged in HeLa cells. The purification retrieved all core subunits of the

complex, but not the deadenylases (67). However, all these efforts failed to broaden our understanding of CNOT10 and detailed studies are still missing.

III.3.3.1. Regulation of the major deadenylation complex CCR4-CAF1-NOT

The major deadenylation complex, CCR4-CAF1-NOT, triggers mRNA degradation and hence it is important to control the activity of this complex. One level of regulation is given by the protection of the poly(A) tail, by poly(A) tail binding proteins (PABPs). In order to start deadenylation and trigger mRNA decay, PABPs need to be removed from the poly(A) tail (72, 84, 85). *In vitro* studies in yeast have shown that the CCR4-CAF1-NOT complex alone was not able to deadenylate mRNAs that were protected by poly(A) binding protein 1 (85). Thus, proteins that modulate the abundance of PABP on mRNAs can potentially regulate the initial step of mRNA degradation. Another way to control the activity of the major deadenylation complex is by preventing its attachment to mRNAs. Stress granules in eukaryotes were identified as places in the cytoplasm that do not contain deadenylases (86, 87). In addition to being in different places in the cell, the human NOT complex exhibits a tissue specific expression pattern, which might help to regulate the abundance of transcripts in different tissues (69, 88).

The CCR4-CAF1-NOT complex can directly be recruited to mRNAs by a variety of RNA binding proteins. In human cells the complex can be recruited by GW182/TNRC6 to mRNAs targeted to microRNA-induced mRNA decay (75, 89). It was also shown that the complex could be recruited by the interaction of NOT1 and Tis11 proteins so as to mediate degradation of mRNAs with AU-rich elements (74). In yeast, PUF proteins were shown to recruit the CCR4-CAF1-NOT complex to mRNAs by interacting with both deadenylases of the complex (90-92). For instance, it is known that the RNA-binding protein Mpt5p (PUF family member) recruits Pop2p (CAF1), Dhh1p and Dcp1p to *HO* transcripts and thereby triggers their degradation. The deletion of Mpt5p reduced deadenylation of *HO* transcripts and stabilised them (90). In Drosophila, studies have shown that the RNA-binding proteins Smaug and Nanos (both important for proper segmentation of Drosophila

embryos) interact with the CCR4-CAF1-NOT complex and hence trigger deadenylation as well as degradation of target mRNAs (93-96). Moreover, the RNA-binding protein Bicaudal-C (Bic-C) is required for the maternal pattering of Drosophila embryos. It was shown that Bic-c directly interacts with NOT3/5 and thereby recruits the deadenylation complex to promote deadenylation (97). Finally, the family of BTG/Tob proteins has been implicated in the recruitment of the CCR4-CAF1-NOT complex (98). This family of proteins is unique to metazoans (98) and several of its members have been found to interact with CNOT7 and 8 (99, 100).

It is important to note that these mechanisms are not mutually exclusive but can act together in order to control the function of the complex.

III.4. XRN1

XRN1 is a cytoplasmic exonuclease responsible for the degradation of 5' monophosphorylated mRNAs. Recently the structure of XRN1 has been resolved for *D. melanogaster* (Pacman) (101) and *Kluyveromyces lactis* (102). The studies show that the active pocket from XRN1 cannot accommodate larger 5' groups, which explains why XRN1 is not able to digest capped mRNAs. Other studies could establish that XRN1 is involved in miRNA-induced mRNA degradation (103), small interfering RNA-mediated decay (104) and nonsense-mediated decay (105). In *Saccharomyces cerevisiae*, disrupting the XRN1 gene resulted in a reduced growth rate (106), an increased cell size as well as a variation in mRNA and protein levels (107). Genome-wide transcription studies using RNAseq with knockout mutants of XRN1 in yeast, revealed a new class of XRN1-sensitive antisense regulatory non-coding RNAs, called XUTs (108). A similar approach showed that XRNA, XRN1's homologue in *T. brucei*, is involved in the degradation of unstable RNAs (8).

III.5. Exosome

In yeast and other eukaryotes, the exosome is a multi-protein complex that consists of 9 core subunits (Rrp41/Ski6, Rrp42, Rrp43, Rrp45, Rrp46, Mtr3p

and Rrp4, Rrp40 and Csl4), its associated catalytic subunits Dis3/Rrp44 (endo- and exonucleolytic activity) and Rrp6 (exonucleolytic activity) (109-112). In the nucleus of yeast, Rrp6 and Dis3/Rrp44 are associated to the exosome core subunits whereas in the cytoplasm, the only attached catalytic subunit is Dis3/Rrp44. In human, three different homologues of Rrp44 (H1, H2, and H3) have been identified and it is suspected that their use might vary (113). The core complex consists of six potential RNase-PH-like subunits (Rrp41/Ski6, Rrp42, Rrp43, Rrp45, Rrp46, Mtr3p), which form a ring-like structure and are not enzymatically active due to the lost of key residues, important for RNA binding or for metal and phosphate coordination (111, 113). The three RNA-binding proteins (Rrp4, Rrp40 and Csl4) sit as a trimeric cap on top of the hexameric ring (111). In the nucleus, the exosome interacts with other complexes (e.g. TRAMP (Trf4–Air2–Mtr4 polyadenylation) complex) and is involved in RNA processing, RNA surveillance and degradation of unstable transcripts (114, 115). In yeast, it was shown that the TRAMP complex polyadenylates and unwinds RNAs, which stimulates degradation by the exosome (114, 116). In the cytoplasm, the exosome functions mainly in normal and ARE-mediated decay (AMD), but is also implicated in 3' degradation in no-stop decay (NSD=mRNA without termination codon), no-go decay (NGD=mRNA with sequence hindering ribosome translocation) and nonsense-mediated decay (NMD=mRNA with premature termination codon) (115).

III.6. RNA interference and miRNAs

RNA interference evolved in order to degrade viral RNAs and transposable elements, and consequently act as an innate nucleic-acid-based immune response (117, 118). Two main classes, siRNA and miRNA, have evolved in order to suppress harmful RNAs. Despite being functionally equivalent, they differ in their biogenesis. Micro RNAs result from transcripts in the nucleus that form stem-loop structures, whereas siRNA originate from long double-stranded RNA (dsRNA) precursors. The later can be from either endogenous or exogenous resources (119). The process of miRNA-induced mRNA decay involves the binding of a small RNA (20-25 nt) protein complex (RISC) to the

3'UTR of their mRNA target. Besides being targeted to deadenylation followed by decay, mRNAs can also be repressed in translation or cleaved when bound by the miRNA/RISC complex, (119, 120).

III.7. RNA granules: P-bodies and Stress granules

mRNAs are coated by proteins in order to be processed, exported, translated or degraded. The complexes consisting of mRNAs and proteins are called messenger ribonuleoprotein (mRNP) complexes. In the cytoplasm, mRNPs that are removed from the translationally active pool are degraded in the 5' direction after deadenylation in so-called processing bodies (P-bodies) (121). P-bodies are constitutive RNA granules that contain deadenylases, the 5'-3' degradation machinery, translation initiation factors and components of the NMD and miRNA pathways, but lack the exosome (121). For instance, Ccr4 was identified as a component of P-bodies and shown to be essential in their formation in HeLa cells (122, 123). It is also speculated that in P-bodies, mRNPs can be stored until further use (121, 124, 125).

Upon stress, another type of granule can be observed in the cytoplasm of most eukaryotic cells, the so-called stress granules. They depend on the presence of P-bodies and silent mRNPs can shuttle between these foci. They contain the small ribosomal subunit (40 S), several translation initiation factors, poly(A)-binding protein and RNA-binding proteins (e.g. TIA-1), indicating that the contained mRNPs were stalled in translation initiation, before being shuttled in stress granules (126). The function of stress granules is not well understood yet, but they are believed to serve as storage foci for the duration of stress (126).

III.8. Trypanosomiasis

There are two subspecies responsible for Human African Trypanosomiasis (HAT): *T. b. gambiense* and *T. b. rhodesiense*. HAT is also known as African sleeping sickness and is found in sub-Saharan Africa where more than 60 million inhabitants are at risk of being infected. However, recent efforts to prevent African sleeping sickness reduced the reported cases of annual infections from around 50,000-70,000 to below 10,000 (127, 128, http://www.who.int/mediacentre/factsheets/fs259/en/, June 2012). This being said, it is fundamental to emphasise the fact that most cases remain unreported.

The parasites are transmitted by the tsetse fly, which belongs to the family of Glossinidae. Upon infection the parasite first proliferates in the bloodstream and once a certain density is reached, it crosses the blood-brain barrier. It evades the host immune system through frequent changes of their surface coat enabled by antigenic variations of the variant surface glycoprotein (VSG). Clonal variants within the population of bloodstream form trypanosomes account for the fact that a subpopulation of *T. brucei* always persists clearance by the immune system. Once the central nervous system is infected, patients start to show neurological disorders and finally fall into coma. If the disease remains untreated, most cases will result in death.

Up to 95% of the reported cases of African sleeping sickness are caused by *T. b. gambiense,* which is mainly found in West Africa (http://www.who.int/mediacentre/factsheets/fs259/en/, June 2012). The disease caused by *T. b. gambiense* leads to a chronic infection that can last for several years. In East Africa, the responsible causative agent is *T. b. rhodesiense* and leads to a more acute form of the disease. A third subspecies, named *T. b. brucei*, is used in laboratories since it is commonly not infectious for humans but mainly for game and wild animals. In this case, the disease is called Nagana. However, the main threat for African lifestock is not *T. b. brucei* but *T. congolense* and *T. vivax*.

The life cycle of *T. brucei* starts when the Tsetse fly takes a bloodmeal during which the non-proliferative stumpy form of the parasite is ingested. In the midgut, *T. brucei* differentiates into the proliferative procyclic form and

migrates first to the proventriculus and then to the salivary glands, where it finally transforms into the infectious metacyclic form. During the next blood meal, the metacyclic parasite enters the bloodstream of its new host and differentiates into the long slender bloodstream form of the parasite. Once a certain density is reached, the parasite transforms into the short stumpy form, which is infectious for tsetse flies.

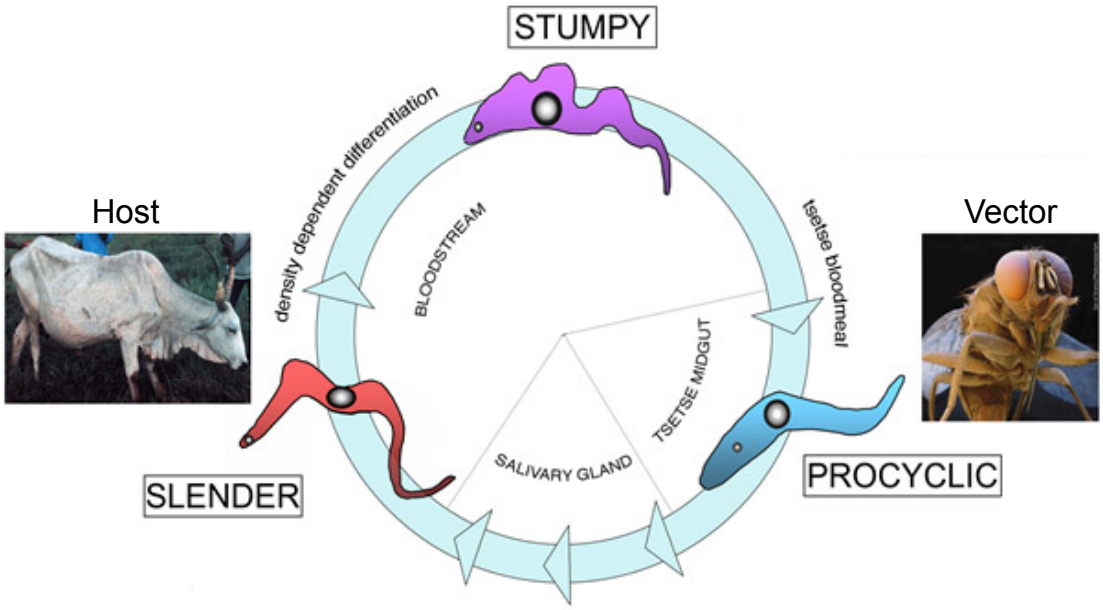

Figure 3 Simplified life cycle of *T. brucei brucei*

The figure shows a simplified overview of the life cycle of *T. b. brucei.* After reaching a certain density in the bloodstream of its host, the parasite differentiates from the long slender to the infectious short stumpy form. During the bloodmeal, the tsetse fly ingests the parasite, which transforms into the procyclic form in the fly's midgut. It then migrates from the midgut to the salivary gland and changes there to the infectious non-proliferative metacyclic form. During the next blood meal, the metacyclic parasite is transmitted. (Picture taken and modified from: http://www.biology.ed.ac.uk/research/groups/kmatthews/index.htm, June 2012)

For this study, I mainly used the monomorphic long slender bloodstream and procyclic form parasites for some experiments. Both can be easily cultured in a lab.

III.9. Gene regulation in trypanosomes

Due to the high diversity of its environment, the parasite is obliged to change its gene expression rapidly in order to survive (129). Compared to other model organisms like yeast and *Drosophila*, the regulation of gene expression is very different in *T. brucei*. Protein-coding genes are arranged in large polycistronic units, transcribed by RNA polymerase II (130). The maturation of precursor mRNA includes *trans* splicing of the downstream mRNA, which is coupled with polyadenylation of the upstream mRNA (131). During the process of *trans* splicing, a capped 39 nt long spliced leader RNA is attach to every 5' end. The spliced leader gene is the only gene shown to have a clear defined Pol II promoter and a corresponding transcription factor tSNAP42 (132). However, there are reports showing that some sequence loci (e.g. actin and HSP70) can act as promoters but the precise sequence could not be identified yet (133, 134). Thus, the parasite lacks transcriptional control and is dependent on post-transcriptional regulation mechanisms (135).

In order to supply sufficient amounts of mRNA transcripts of highly expressed proteins, the genome contains several copies of certain genes (e.g. histone H4, tubulin etc.), and RNA polymerase I transcribes the surface proteins VSG (variant surface glycoprotein) and EP (procyclin) in addition to rDNA (136). Epigenetic mechanisms suppress all VSG copies in the genome except the active one (137).

Another mechanism to control the amount of mRNA transcript in the cell is the use of RNA binding proteins. Several groups exist in *T. brucei*, which can bind to the cis-element(s) of their target mRNAs and thereby stabilise or destabilise them. The biggest group is that of RNA Recognition Motif (RRM) proteins. In *T. brucei*, this group consists of 75 proteins and each of them possesses one or more motifs in their amino acid sequence (138). Most of them have no identifiable orthologues in other eukaryotes, but are *T. brucei*-specific, like RBP3 or RBP10 (139, 140). Proteins with CCCH zinc finger motifs bind to single stranded RNA and were found to be implicated in differentiation and stress response (141). PUF (Pumilio/Fem-3-binding factor)-domain-containing proteins form one of the major known groups of RNA binding proteins in trypanosomes. There are at least 10 Puf proteins identified

in *T. brucei* that lead to stabilisation or destabilisation of its mRNA target or are involved in rRNA processing (142). For instance, PUF9 neutralises a destabilising mRNA element by binding to it (143) and PUF7 was shown to be involved in pre-rRNA processing (144). The latest identified group of RNA binding proteins in trypanosomes are the ALBA proteins. Four different proteins of this group have been identified and it was shown that they could interact with the translation machinery (145). Their exact function, however, is still unknown.

Given the dependence of *T. brucei* on the post-transcriptional control mechanisms detailed above, the parasite reveals itself as an ideal model organism to study them.

III.10. mRNA degradation in *T. brucei*

T. brucei have most of the common mRNA degradation pathways. It was shown that the parasite lacks transcriptional control for protein-coding genes and has all-important enzymatic homologues for mRNA decay. This makes it an optimal model organism to study mRNA turnover.

In the parasite, mRNA degradation starts with deadenylation (8) and cell extracts revealed decapping activity, but the responsible enzyme could not be identified so far (146). It has been shown that degradation could proceed from both ends (58, 147): from the 3' direction by the exosome together with the decapping scavenger and from the 5' directions by XRNA, the trypanosome homologue of XRN1.

The CAF1-NOT complex was identified as the major deadenylation complex. A tandem affinity purification of CAF1 could pull-down NOT1, 2, 3/5 and DHH1. Additionally, CAF130/CNOT10- and CAF16-like proteins were retrieved from the affinity purification. The study also revealed that *T. brucei* does not contain a homologue of CCR4. Depleting NOT1, CAF1 and DHH1 in bloodstream form parasites inhibited growth and led to death after 2 – 3 days of RNAi induction. CAF1 was identified as the major deadenylases based on the following observations. The knockdown of CAF1 inhibited deadenylation of bulk mRNAs and mRNA degradation assays showed a delayed decay of all analysed mRNAs. Interestingly, upon CAF1 depletion, only the steady-state

level of *EP*, an mRNA transcribed by RNA Pol I, was elevated but this was not the case for the investigated mRNAs, which are transcribed by RNA Pol II (38, 58). Two different explanations have been provided to account for this fact: there might either be an inhibitory feedback response from RNA polymerase II or mRNA synthesis depends on ribonucleotides produced by mRNA degradation (38, 58).

Along with the CAF1-NOT complex, the parasite has two other deadenylases: PAN2 and PARN-1 (58, 148). In trypanosomes, PAN2 appears to be essential for growth but, in contrast to yeast and mammalian cells, PAN2 activity in *T. brucei* does not seem to depend on PAN3. A knockdown of PAN2 did not affect the mRNA degradation kinetics of several mRNAs (58). It was proposed that PARN-1 participates in the regulation of stage specific mRNAs, but the results were not clear (148).

The major homologue of XRN1 in *T. brucei* is XRNA, which plays an important role in 5' – 3' degradation, and in particular that of unstable mRNAs (8).

T. brucei possesses a functional exosome that is similar to its orthologues in yeast and humans (149). All subunits are essential for growth and rRNA maturation, except RRP6. Trypanosome RRP6 is not restricted to the nucleus and could be detected in the cytoplasm in stoichiometric amounts (147, 150-152). Moreover, there is no evidence of the TRAMP complex's presence. Although, the trypanosome RNA helicase *Tb*MTR4 is essential for growth and rRNA maturation, it does not interact with the exosome and *Tb*NPAPL, a putative homologue of Trf4p, nor does it interact with other RNA-binding proteins. (153).

A "classical" nonsense mediated decay (NMD) pathway still needs to be confirmed since experiments trying to reverse a putative NMD effect by depleting UPF1 have failed (154).

III.11. RNA granules in *T. brucei*

Trypanosomes, like other eukaryotes, possess RNA granules in their cytoplasm. A P-body-like structure could be identified in *T. cruzi,* by detecting XRNA and DHH1 in discrete foci (155-157). UBP1 and PUF6 were also

identified in the P-bodies of *T. cruzi* along with translation initiation factors (155). In *T. brucei*, DHH1, XRNA and SCD6 were found in discrete foci considered to be P-bodies. However, none of the other common P-body markers could be analysed due to a lack of antibodies (157). Upon heat shock, stress granules were identified in *T. brucei* and *T. cruzi*. In *T. brucei,* translation initiation factors eIF4E (1 to 4), eIF2α and eIF3B as well as both poly(A)-binding proteins PABP1 and PABP2 could be identified in discrete foci after stress induction (157). The role of these granules in trypanosomes is not well understood.

IV. Materials and Methods

Some parts of this section were copied from the PhD thesis of Angela Schwede and Corinna Benz.

IV.1. In silico experiments

To find potential homologues of *Tb*927.10.8720, the protein sequence was analysed by BLASTp, psi-BLAST and tBLAST (158). I used standard parameters and excluded kinetoplastids (taxid:5653) from the search. Domains were identified by a SUPERFAMILY search (159). Multiple sequence alignments were done with ClustalW, to find conserved regions in protein sequences. For in silico cloning the Lasergene software package from DNASTAR was used.

IV.2. Cell culture

The experiments were done with bloodstream form *Trypanosoma brucei* that stably express the tetracycline repressor, with or without T7 polymerase expression. Culturing, transfections and RNAi experiments were conducted as described earlier (160). mRNA decay was analyzed after 24 hours of RNAi targeting CNOT10. Cells were treated with Sinefungin (final concentration 2 µg/ ml) for 5 min, and then Actinomycin D was added to a final concentration of 10 µg/ml. The experiment was conducted as described in (38).

Sahil Sharma did all experiments in human cells. HEK293 cells were cultured in Dulbecco's modified Eagle medium (DMEM) containing 10% fetal bovine serum (PAA Laboratories), 2 mM l-glutamine, 100 U/ml penicillin, and 0.1 mg/ml streptomycin (all PAN Biotech) at 37°C/5% CO_2. Cells were transfected with DNA using polyethyleneimine (PEI) (Polysciences Europe; 1 mg/ml, pH 7.0) at a ratio of 1:2 (DNA:PEI) in serum-free DMEM without antibiotics. For transfection of siRNAs, Lipofectamine RNAimax (Invitrogen) and Optimem (Gibco) were used according to the manufacturer's protocol.

The below-mentioned siRNAs were transfected at a concentration of 100 nM with Lipofectamine 2000 twice over a time period of 4 days:

C2/S014 (control): 5′-GGUCCGGCUCCCCCAAAUGdTdT-3′
S021 (CNOT1): 5′-GGAACUUGUUUGAAGAAUAdTdT-3′
S059 (CNOT10): 5′-CAGCGAAAGCAGTGAAACTdTdT-3′

The medium was changed to regular DMEM 4 h after transfection of DNA.

IV.3. RNA extraction and Northern Blot analysis

Total RNA was extracted using peqGold Trifast (peqLab, Germany). RNA was run on formaldehyde gels and blotted onto Nytran membranes (GE Healthcare). Northern blots were hybridized with radioactively labelled DNA (Prime-IT RmT Random Primer Labelling Kit, Stratagene) or RNA (MAXIscript, Ambion) probes (38). Northern blots used for spliced leader experiments, were prehybridized for 2 h at 42°C in 6xSSC, 0.5% SDS, 5x Denhardt, 0.05 % sodium pyrophosphate and 100 µg/ml boiled herring sperm DNA. For hybridization the P^{32} labelled anti-sense oligo of the spliced leader sequence cz4490 was added to the prehybridisation solution o/n at 42°C. The blot was first washed twice at RT for 15 min and once for 1 h with 6xSSC, 0.05% sodium pyrophosphate, after the blot was washed for 30 min at 55°C in 6xSSC, 0.05% sodium pyrophosphate. Signals were measured using a phosphorimager (Fuji, FLA7000). Either the signal of the signal recognition particle (*7SL*) or a large subunit rRNA (*LSU1*) was used for normalization. The half-lives were estimated using only the segments of the time course that gave exponential decay curves (fitted with a linear correlation coefficient generally exceeding 0.9).

RNA used for RNAseq was treated with the RiboMinus™ Eukaryote Kit (Invitrogen), in order to remove the rRNA from the sample. All steps were done as described in the kit and eluted in 16 µl. The RNA was sent to the Deep Sequencing Core Facility of the Bioquant, Heidelberg. The received data was analysed by Abeer Fadda.

IV.4. Cloning

All experiments (PCR, restriction, ligation, transformation, sequencing, agarose gels, etc.) necessary for cloning were conducted as described in the TDR/EMBO protocol or as stated in the instruction of the manufacturer. For restriction reactions enzymes from NEB were applied. In order to blund a vector, T4 polymerase from NEB was used. For dephosphorylation of linearised plasmids Antarctic Phosphatase (NEB) was deployed. For normal control/ colony PCRs GoTaq® DNA Polymerase from Promega was used and for all PCRs for cloning reactions Phusion® High-Fidelity DNA Polymerase from Finnzymes was deployed. For plasmid DNA purification and Nucleic Acid gel extraction the kits from Macherey-Nagel were used. To purify genomic DNA, I harvest around $1x10^8$ BS trypanosomes and used the illustra™ tissue & cells genomicPrep Mini Spin Kit from GE Healthcare and followed the instructions of the manufacturer. The list of plasmids and primers used in this thesis is at the end of this chapter.

IV.5. Co-Immunoprecipitation

For co-Immunoprecipitation (co-IP) experiments $5x10^7$ trypanosomes were lysed in co-IP-lysis buffer containing 10mM NaCl, 10mM Tris-HCl, pH7.5, 0.3 % IGEPAL and protease inhibitors (Protease Inhibitor Mixture (EDTA-free); Roche Applied Science) by passing them 5 times through a 27 g syringe. To test RNA dependent interaction, RNaseA was added to the lysis and wash buffer at a concentration of 200 µg/ml and as a control recombinant RNasin® Ribonuclease inhibitor (Promega) at a concentration of 48 µg/ml. Afterwards the cells were centrifuged for 20 min at 4°C, 16 x g. 30 µl of V5 Antibody or c-myc Antibody coupled agarose slurry (both Bethyl) were washed 4 times with 1xPBS and once with co-IP lysis buffer adjusted to 180 mM NaCl at 4°C, 0.9 x g for 2.00 min. The cell supernatant was transferred into a new tube and the salt concentration was adjusted to 180 mM NaCl. A sample of $5x10^5$ cells was taken from the input and 2x Laemmli buffer was added. Beads and cell lysates were incubated for one to 1.5 h at 4°C with rotation. A sample

equivalent to $5x10^5$ cells was taken from the supernatant and 2x Laemmli buffer was added to it. The beads were washed four times for 5 min at 4°C with salt-adjusted lysis buffer then boiled in 2x Laemmli buffer.

Twenty-four hours after transient transfection, HEK293 cells from a confluent 10 cm dish were collected and lysed in 400 µl ice-cold RNA-IP lysis buffer (50 mM Tris [pH 8.0], 150 mM NaCl, 1 mM $MgCl_2$, 2 % NP-40, 10% glycerol with freshly added protease inhibitors [Complete; Roche]). Nuclei were removed by centrifugation at 500 × *g* for 5 min at 4°C. A total of 30 µl of Streptavidin sepharose beads (GE Healthcare) were added for an additional 1.5 - 2 h and washed six times in NET2 buffer (50 mM Tris [pH 7.5], 150 mM NaCl, 0.5% Triton X-100). Protein complexes were eluted with 50 µl SDS sample buffer with 100 mM dithiothreitol (DTT). Proteins were resolved on 5 – 20 % gradient polyacrylamide gels and transferred onto a 0.2-µm-pore-size nitrocellulose membrane (Peqlab) for Western blotting. Horseradish peroxidase-coupled secondary antibodies (Jackson Immunoresearch) in combination with Western Lightning enhanced chemiluminescence substrate (Perkin Elmer) were used for detection. Streptavidin sepharose beads (GE Healthcare) were used to purify myc-Strep-tagged (myc-SG) proteins.

IV.6. Two-hybrid Analysis

Esteban Erben conducted all yeast two-hybrid experiments. Complete ORFs were cloned into pGADT7 (GAL4 activation domain vector) and pGBKT7 (GAL4 DNA-binding domain vector) (Matchmaker 3 System, Clontech). The two-hybrid yeast strain AH109 was then transformed with these plasmids in all possible combinations. The expression of the fusion protein was confirmed by Western blot analysis using antibodies directed against the HA epitope of GAL4 activation domain fusion proteins and anti c-Myc antibody to detect GAL4 DNA-binding domain fusions. Transformants were selected on four drop-out SD/-Trp/-Leu/-His/-Ade culture plates after 4 days of incubation at 30°C, and the resulting positive clones were assayed for β-galactosidase activity using a colony-lift filter assay. Alternatively, reporter activation was tested by replica plating on three drop-out SD/-Trp/-Leu/-His (medium stringency). As negative control for self-activation, we used a

combination of the Not1-complex subunits with CLONTECH vectors pGAD-T-antigen and pGBKT7-p53. Further, p53 (pGBKT7-p53) and SV40 large T-antigen (pGADT7-T) cotransformants were used as positive controls, whereas lamin C (pGBKT7-Lamin) and pGADT7-T cotransformants were used as negative controls.

IV.7. Glycerol Gradient

$3x10^7$ bloodstream trypanosomes or HEK293, cells from a confluent 10 cm dish, were washed with 1xPBS, then frozen in liquid nitrogen and stored at -80°C until use. The cell pellets were thawed on ice and resuspended in ice-cold buffer containing 10mM Tris-HCl, pH 7.6, 10 mM NaCl, 10 mM MgCl and protease inhibitors (Protease Inhibitor Mixture (EDTA-free); Roche Applied Science), then forced 5 times through a 27 g needle. Igepal CA-630 (Sigma) was added to a final concentration of 0.1% and the cells were again forced through the needle 5 times. The lysate was centrifuged first for 20 min at 4°C, 10,000 x g, followed by an additional spun for 1 h at 100,000 x g at 4°C. The supernatant was layered onto a 12 ml 10-30% glycerol gradient (200 mM KAc, 20mM Tri-HCl, pH 8,0, 5 mM MgAc, 1mM DTT and protease inhibitors (Protease Inhibitor Mixture (EDTA-free); Roche Applied Science), which was then spun at 229,900 x g for 17 h at 4°C. 27 fractions were then taken from the top at 23 second intervals. The fractions were incubated on ice overnight with 15% TCA, 0.1% DOC and 10 µg BSA. Precipitations were washed with acetone and resuspended in Laemmli buffer.

IV.8. Tandem Affinity Purification

In total, $2.5x10^{10}$ bloodstream trypanosomes, with *in situ* N-terminal protein-A-calmodulin-binding-peptide tagged CNOT10, were harvested and used for tandem affinity purification as previously described (150). The eluate was run one centimetre in a 10% SDS-PAGE resolving gel and stained with colloidal coomassie. The whole preparation was then send for mass spectrometry.

IV.9. Protein detection

Trypanosoma BSF or HEK cells were washed once with PBS and after dissolved in 2X Laemmli Buffer. Protein samples were run on a SDS-PAGE and after blotted onto an Optitran BA-S 85 Reinforced NC 0.45 µm membrane (Whatman, Dassl, Germany). The Blots were probed with either Anti-V5 (1:2000; 5% Milk in TBS-T) or Anti-myc primary Antibody (1:2000; 5% Milk in TBS-T) and Anti-mouse secondary Antibody (1:2000; 5% Milk in TBS-T). After, blots were developed with Western Lightning®-ECl solution from PerkinElmer.

Immunofluoresence (IF) microscopy was conducted as described earlier in Schwede et al. 2008 (38).

The following antibodies were used in Western blotting:

Monoclonal mouse Anti-V5 (Santa Cruz), monoclonal mouse anti c-myc (Santa Cruz), monoclonal mouse anti GFP (Santa Cruz), ECL™Anti-Rabbit IgG (GE Healthcare), ECL™Anti-Mouse IgG (GE Healthcare), polyclonal rabbit antibodies anti-myc (A-14, sc-789, Santa Cruz), anti-CNOT10 (15938-1-AP, Protein Tech) and anti-CNOT1 (14276-1-AP, Protein Tech). Polyclonal rabbit anti-CAF1a was kindly provided by Ann-Bin Shyu (University of Texas, Houston, TX). Polyclonal rabbit anti-PUF2 (1:2000).

Table 1: Cloned vectors

pHD No.	*Description*	*Cloning Strategy*	*Primers (cz)*
RNAi			
2300	inducible expresssion with puromycin resistence	pHD1034 backbone (not1-spe1) + pHD1145 insert (not1-spe1, long fragment)	-
2099 (BS)	CAF16 RNAi stem loop (Hygro)	Part of the CAF16 ORF was amplified using following primers cz4684 and cz4685. An aliquot of the PCR fragment was cut with SalI and SpeI and cloned into pHD1144. After, the remaining aliquot of the PCR fragment was cut with EcoRI and BglII and cloned into CAF16partI/pHD1144. The CAF16 stuffer was cut with HindIII and BglII and cloned into pHD1145 linearised with HindIII and BamHI.	4684, 4685
2207 (BS)	CAF40 RNAi stem loop (Hygro)	Part of the CAF40 ORF was amplified using following primers cz4686 and cz4700. An aliquot of the PCR fragment was cut with SalI and SpeI and cloned into pHD1144. After, the remaining aliquot of the PCR fragment was cut with EcoRI and BglII and cloned into CAF40partI/pHD1144. The CAF40 stuffer was cut with HindIII and BglII and cloned into pHD1145 linearised with HindIII and BamHI.	4686, 4700
2205 (BS)	NOT2 RNAi stem loop (Hygro)	Part of the NOT2 ORF was amplified using following primers cz4690 and cz4693. An aliquot of the PCR fragment was cut with SalI and SpeI and cloned into pHD1144. After, the remaining aliquot of the PCR fragment was cut with EcoRI and BglII and cloned into NOT2partI/pHD1144. The NOT2 stuffer was cut with HindIII and BglII and cloned into pHD1145 linearised with HindIII and BamHI.	4690, 4691
2203 (BS)	NOT3/5 RNAi stem loop (Hygro)	Part of the NOT3/5 ORF was amplified using following primers cz4692 and cz4693. An aliquot of the PCR fragment was cut with SalI and SpeI and cloned into pHD1144. After, the remaining aliquot of the PCR fragment was cut with EcoRI and BglII and cloned into NOT3/5partI/pHD1144. The NOT3/5 stuffer was cut with HindIII and BglII and cloned into pHD1145 linearised with HindIII and BamHI.	4692, 4693
2101 (BS)	CNOT10 RNAi stem loop (Hygro)	Part of the CNOT10 ORF was amplified using following primers cz4688 and cz4689. An aliquot of the PCR fragment was cut with SalI and SpeI and cloned into pHD1144. After, the remaining aliquot of the PCR fragment was cut with EcoRI and BglII and cloned into CNOT10partI/pHD1144. The CNOT10 stuffer was cut with HindIII and BglII and cloned into pHD1145 linearised with HindIII and BamHI.	4688, 4689
2102 (PC)	CNOT10 RNAi stem loop (Hygro)	Part of the CNOT10 ORF was amplified using following primers cz4688 and cz4689. An aliquot of the PCR fragment was cut with SalI and SpeI and cloned into pHD1144. After, the remaining aliquot of the PCR fragment was cut with EcoRI and BglII and cloned into CNOT10partI/pHD1144. The CNOT10 stuffer was cut with HindIII and BglII and cloned into pHD1146 linearised with HindIII and BamHI.	4688, 4689
2301 (BS)	CNOT10 RNAi stem	Stuffer fragment from CNOT10 RNAi was cut out using HindIII/BglII and cloned into pHD2300	4688, 4689
1851	PAN2 RNAi	Schwede et al. 2009	-
1843	CAF1 RNAi p2T7TA	Schwede et al. 2008	-
1154	RRP45	Estévez et al., 2002	-
Knockout			
2264	CNOT10 Knock out (Bla)	Part of the 5'UTR of CNOT10 was amplified with cz4032 and 4033. The PCR fragment was cut with XhoI as well as HindIII and subsequnetly cloned into pHD1748. A part of the 3'UTR of CNOT10 was amplified using cz4034 and cz4035. The PCR fragment was cut with XbaI as well as NotI and subsequently cloned into 5'UTRCNOT10/pHD1748 linaerised using the same enzymes.	4032, 4033, 4034, 4035
2265	CNOT10 Knock out (Hygro)	PCR on pHD1145 using following primers, cz4131,cz4132, to retrieve Hygromyin resistance gene. The PCR fragment was cut with HindIII and XbaIas well as pHD2264 to replace the Blasticidin resistance of pHD2264.	4131, 4132

Table 1: Cloned vectors

pHD No.	*Description*	*Cloning Strategy*	*Primers (cz)*
Protein Tags			
1846	N-terminal V5 in situ NOT1	Schwede et al. 2008	-
2211	N-terminal V5 in situ CAF1	Part of the ORF of CAF1 was amplified using cz3921 and cz3922. The PCR fragment was digested with XhoI and ApaI and cloned in the linearised BlaV5 plasmid, cut with the same enzymes as the fragment. After a PCR was done with cz3919 and cz3920 to amplify a part of the 5'UTR of CAF1. The PCR fragment was cut with NotI and XbaI and cloned into the BlaV5 vector that already contained part of the ORF.	3919, 3920, 3921, 3922
2212	N-terminal V5 in situ CNOT10	Part of the ORF of CNOT10 was amplified using cz4715 and cz4716. The PCR fragment was digested with XhoI and ApaI and cloned in the linearised BlaV5 plasmid, cut with the same enzymes as the fragment. After a PCR was done with cz4725 and cz4726 to amplify a part of the 5'UTR of CNOT10. The PCR fragment was cut with NotI and XbaI and cloned into the BlaV5 vector that already contained part of the ORF.	4715, 4716, 4725, 4726
2275	N-terminal V5 in situ CAF40	Part of the ORF of CAF40 was amplified using cz4713 and cz4714. The PCR fragment was digested with XhoI and ApaI and cloned in the linearised BlaV5 plasmid, cut with the same enzymes as the fragment. After a PCR was done with cz4723 and cz4724 to amplify a part of the 5'UTR of CAF40. The PCR fragment was cut with NotI and XbaI and cloned into the BlaV5 vector that already contained part of the ORF.	4713, 4714, 4723, 4724
2309	N-terminal *in situ* TAP tag CNOT10	The plasmid p2676 was cut with HindIII and with T4 polymerase blund ends were generated. After the plasmid was cut with ApaI. Part of the CNOT10 ORF was amplified using cz4491 and cz4716. The PCR fragment was cut with HpaI and ApaI and ligated to the linearised plasmid p2676. After the vector was cut with SacI and NdeI to release the 5'UTR of Hsp70, which was replaced by a part of the 5'UTR of CNOT10, which was before PCR amplyfied with cz4491 and cz4492 as well as cut with SacI and NdeI.	4491, 4492, 4710, 4716
2268	C-terminal myc-tagged CAF1:	The ORF of CAF1 was amplified using following primers cz4705 and cz4706. The PCR fragment was cut with HindIII and BamHI and cloned into pHD1700, which was linearised with the same enzymes.	4705, 4706
2154	His-tag CNOT10	CNOT10 ORF was amplified using cz4701,4702. The PCR fragment was cut with KpnI and BglII and cloned into pQEA38., which was linearised with the same enzymes	4701, 4702
2342	λN-CAF1 C-terminal myc tag	Done by E. Erben in 2011	4422, 4660
2297	GFP + 6x B-Box reporter mRNA	Done by E. Erben in 2012	4327, 4328, 4329, 4330
2338	pGADT7 + Not1 C-terminal fragment NdeI/BamHI	Done by E. Erben in 2011	4428, 4172
2339	pGADT7 + Not1 N-terminal fragment EcoRI/BamHI	Done by E. Erben in 2011	4426, 4427
2340	pGBKT7 + Not1 C-terminal fragment NdeI/BamHI	Done by E. Erben in 2011	4428, 4172
2341	pGBKT7 + Not1 N-terminal fragment EcoRI/BamHI	Done by E. Erben in 2011	4426, 4427
2248	pGBKT7 + CAF1 EcoRI/BamHI	Done by E. Erben in 2011	4077, 4078
2249	pGBKT7 + CNOT10 EcoRI/BamHI	Done by E. Erben in 2011	4079, 4080
2257	pGBKT7 + NOT3/5 NdeI/BamHI	Done by E. Erben in 2011	4081, 4082
2251	pGADT7 + CAF1 EcoRI/BamHI	Done by E. Erben in 2011	4077, 4078
2253	pGADT7 + CNOT10 EcoRI/BamHI	Done by E. Erben in 2011	4079, 4080
2256	pGADT7 + NOT3/5 NdeI/BamHI	Done by E. Erben in 2011	4081, 4082

Table 3: Primers

cz	Name on the tube	Sequence	Restriction site(s)
4684	Caf16_RNAi2_for01	GAGAAGATCTGCATGCGAGCGAATGTTGTTGTGTGG	BglII, SpeI
4685	Caf16_RNAi2_rev01	CGGAGAATTCGTCGACACTGTTGGCCATTCCTGAAG	EcoRI, SalI
4686	Caf40_RNAi2_for01	GAGAAGATCTGCATGCACCTGAGACGCGTGAGAACT	BglII, SpeI
4700	Caf40 RNAi	CGGAGAATTCGTCGACAGGAGCCTCTGCACGATAAA	EcoRI, SalI
4690	Not2_RNAi2_for01	GAGAAGATCTGCATGCGACAGCGCTGCATTTTTGTA	BglII, SpeI
4691	Not2_RNAi_rev01	CGGAGAATTCGTCGACGGTGCAGCAAGGAAAGAATC	EcoRI, SalI
4692	Not5_RNAi_for01	GAGAAGATCTGCATGCCTGGAGAAACGAGGCAACTC	BglII, SpeI
4693	Not5_RNAi_rev_01	CGGAGAATTCGTCGACGATTCTTTTGGGGGACCATT	EcoRI, SalI
4688	CNOT10_RNAi2_for01	GAGAAGATCTGCATGCTCAGCACAACTTAGCCATCG	BglII, SpeI
4689	CNOT10_RNAi2_rev01	CGGAGAATTCGTCGACCCATCAGTGGCATGTGGTAG	EcoRI, SalI
4032	Caf130_5UTR_XhoIfor	GAGACTCGAGAGAGAATTCAGGAGAATAACTGG	XhoI
4033	Caf130_5UTR_HindIIIrev	GAGAAAGCTTTTCTACGTCCCTTCTGTCTC	HindIII
4034	Caf130_3UTR_XbaIfor	GAGATCTAGAAGTTGTTTATGTGGGGTCCTTC	XbaI
4035	Caf130_3UTR_NotIrev	GAGAGCGGCCGCTTGATCATTCCTCCGTTGCTC	NotI
4131	Hygro for HindIII	GTCAAGCTTATGAAAAAGCCTGAACTCACCG	HindIII
4132	Hygro rev XbaI	GAGTCTAGATCTATTCCTTTGCCCTCGGAC	XbaI
3919	Caf1v5 utr for	GAGAGCGGCCGCTCACTGAAAGGAGTTTAAGCG	NotI
3920	Caf1v5 utr rev	GAGATCTAGATTTCCCGTTTCCCGTTTCC	XbaI
3921	Caf1v5 orf for	GAGACTCGAGATGATGCAGTATGGTGGCG	XhoI
3922	Caf1v5 orf rev	GAGAGGGCCCCGGAAGTTGAACTGCCAC	ApaI
4715	Caf130_V5_ORF_for01	ACGTCTCGAGATGACGGATGATGTCTTGAGAC	NotI
4716	Caf130_V5_ORF_rev01	ACGTGGGCCCCATTGAGCTTCTCGGAAAGAAC	XbaI
4725	Caf130_V5_5'UTR_for01	ACGTGCGGCCGCGCGCCATTCCTGCTTTCTTC	XhoI
4726	Caf130_V5_5'UTR_rev01	ACGTTCTAGATTCTACGTCCCTTCTGTCTCA	ApaI
4713	Caf40_V5_ORF_for01	ACGTCTCGAGATGCACCAAACCCAAGCGTATT	NotI
4714	Caf40_V5_ORF_rev01	ACGTGGGCCCCCTTCATTCATCCCACGGAG	XbaI
4723	Caf40_V5_5'UTR_for01	ACGTGCGGCCGCGTTGTTTTCCCCATCACAGAG	XhoI
4724	Caf40_V5_5'UTR_rev01	ACGTTCTAGAGGTCACGAAAATCCTCTACAAA	ApaI
4491	5'UTRC130_SacIfor01	ACTGGAGCTCGCGCCATTCCTGCTTTC	SacI
4492	5'UTRC130_NdeIrev01	ACTGCATATGTTCTACGTCCCTTCTGTC	NdeI
4710	Caf130mycNHpaIfor01	GAGAGTTAACATGACGGATGATGTCTTGAG	HpaI
4705	Caf1mycCHindIII for01	GAGAAAGCTTATGATGCAGTATGGTGGCG	HindIII
4706	Caf1mycCBamHI rev01	GAGAGGATCCGCTATGACCCTTTACCGC	BamHI
4701	Caf130KpnIHTagNfor01	GAGAGGTACCATGACGGATGATGTCTTGAG	KpnI
4702	Caf130BglIIHTagNrev01	GAGAAGATCTTCATGCGCACCATGAAAGC	BglII
4422	Caf1	ATAGGGCCCATGCAGTATGGTGGCG	ApaI
4660	Caf1	ATACTCGAGGCTATGACCCTTTACCGC	XhoI
4426	Not1-Nter	GCGGAATTCTTGTATGAGCATACTACTGACAT	EcoRI
4427	Not1-Nter	AGTGGATCCGCACATCGTGATACTCCT	BamHI
4428	Not1-Cter	ATGCATATGGGTGAGGTGTTG	NdeI
4172	Not1-Cter	TATGGATCCCTTCTTGCCTTGAGTTGCG	BamHI
4077	Caf1	TGGAATTCATGATGCAGTATGGTG	EcoRI
4078	Caf1	AAGGATCCTCAGCTATGACCCTTTA	BamHI
4079	Caf130	CGGAATTCATGACGGATGATGTCTTG	EcoRI
4080	Caf130	TAGGATCCTCATGCGCACCAT	BamHI
4081	Not5	GCCATATGATGACAAATAATAAAAAG	NdeI
4082	Not5	GGATCCTCAACGCAGCTC	BamHI
4276	GFP - control mRNA	AAGGGCCCATGGTGAGCAAGGGC	ApaI
4277	GFP - control mRNA	ATCTCGAGGCGGTAACGCTTGTACA	XhoI
4278	GFP - reporter mRNA	ATTCTAGACCGGGCTGCACG	XbaI
4279	GFP - reporter mRNA	TCGCTAGCTTACTTGTACAGCTCGTCCATG	NheI
4327	B-box - reporter mRNA	AAGGATCCTCCCTAAGTCCAACTACTAAACTG	BamHI
4328	B-box - reporter mRNA	AGGAGCTCCCCTAGAGATAATATCCTCGA	SacI
3963	cz3963 Tapseqprimer	CCGAAAGTAGACGCGAATTG	-
4490	SL antisense 39-mer	CAATATAGTACAGAAACTGTTCTAATAATAGCGTTAGTT	-

V. Results

V.1. *Tb*927.10.8720 is an orthologue of CNOT10 in other eukaryotes

The protein encoded by the trypanosome locus *Tb*927.10.8720 was previously identified as a potential component of the CAF1-NOT complex through tandem affinity purification of CAF1 (38). It was shown to be a distant relative of CNOT10 with poor likelihood. The CNOT10-like protein (*Tb*CNOT10) in *T. brucei* comprises 555 amino acids and includes Tetratricopeptide repeat (TPR)-like domains positioned from amino acid 199-313 and 471-550. Analyses of *Tb*CNOT10 by reciprocal blastp and PSI-BLAST permitted to identify more than 40 orthologues of CNOT10 in plants and animals with E-values ranging from 3e-04 to 1e-07. Reciprocal blastp of human CNOT10 (*Hs*CNOT10) against the trypanosome genome yielded *Tb*927.10.8720 as the best match (E value 3e-04). The sequence coverage was between 20 – 60% and depending on the percentage of coverage, identities varied from 20 – 30%. Most of the hits against CNOT10 covered the beginning of the TPR domain of *Tb*CNOT10 and the rest aligned to the beginning until the end of the TPR domain. The sequence alignment comparing the human and trypanosome CNOT10, made with ClustalW, is shown in Figure 4 along with a simplified illustration. A directed BLASTp search in different eukaryotic phyla and kingdoms revealed that CNOT10 could not be detected in Apicomplexa, Diplomonadida, Alveolates and fungi. On the other hand, CAF130 is restricted to fungi and has no orthologues in other kingdoms.

The sequence analyses suggested that *Tb*927.10.8720 might be an orthologue of CNOT10 and will consequently be called *Tb*CNOT10 from now on. My next step was then to prove that *Tb*CNOT10 is a stable member of the NOT complex.

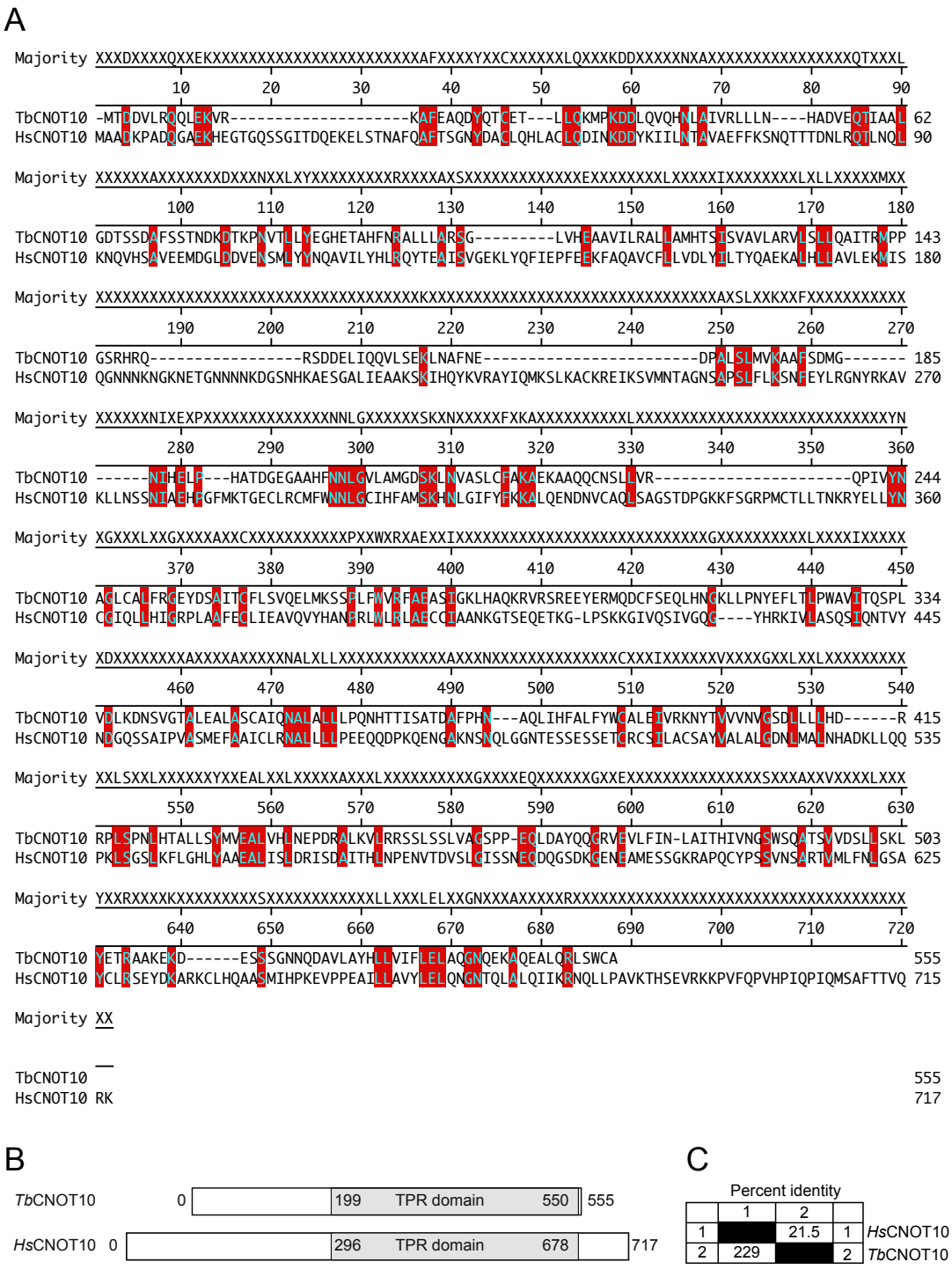

Figure 4 Sequence alignment of human and trypanosome CNOT10

(A) *Hs*CNOT10 was aligned with the potential homologue of *T. brucei* using ClustalW. Amino acids that are conserved between species are shown in red. **(B)** shows a schematic sequence alignment of human and trypanosome CNOT10. The grey colour indicates the sequence area containing the TPR domain. The numbers represent the amino acid residue that corresponds to this area. **(C)** Sequence distance of the ClustalW alignment.

V.2. *Tb*CNOT10 is a member of the CAF1-NOT complex in *T. brucei*

To confirm that *Tb*CNOT10 is a member of the CAF1-NOT complex, I conducted co-immunoprecipitations with *in situ* N-terminal V5-tagged CNOT10 (V5-CNOT10) and inducible C-terminal myc-tagged CAF1 (CAF1-myc). The pull-down of V5-tagged CNOT10 resulted in a coprecipitation of CAF1-myc (Figure 5 A) and was replicable vice versa. RNase A treatment did not disrupt the interaction and confirmed its RNA independency (Figure 5 B).

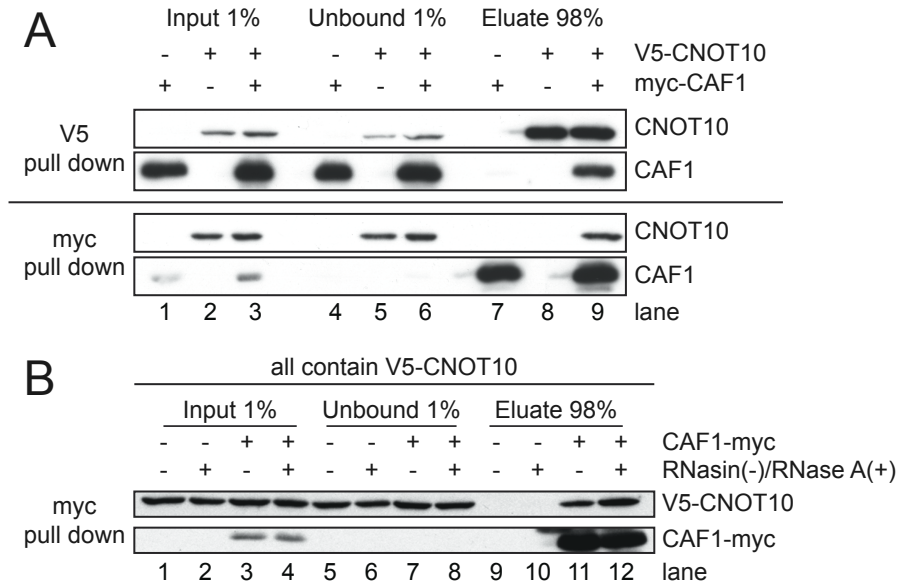

Figure 5 CNOT10 is a member of the CAF1-NOT complex

(A) Immunoprecipitation of V5-CNOT10 resulted in a coprecipitation of CAF1-myc, the experiment was replicable vice versa. **(B)** myc-tagged CAF1 was pulled down in the presence of RNase inbibitor (-) or RNase A (+) and the Western Blot was probed to detect V5-CNOT10.

In order to identify further interaction partners, I tandem affinity purified (TAP) CNOT10. Thus, I created a TAP-tagged CNOT10 cell line by introducing a N-terminal TAP-tag directly upstream of the open reading frame by homologous recombination. The functionality of the tagged-protein was confirmed by knocking-out the remaining wild-type gene (Figure 6 A, A', B-D). The cells were viable and did not show any morphology defects. Proteins resulting from the tandem affinity purification were resolved on a SDS-PAGE and analysed by mass spectrometry (Figure 6 E).

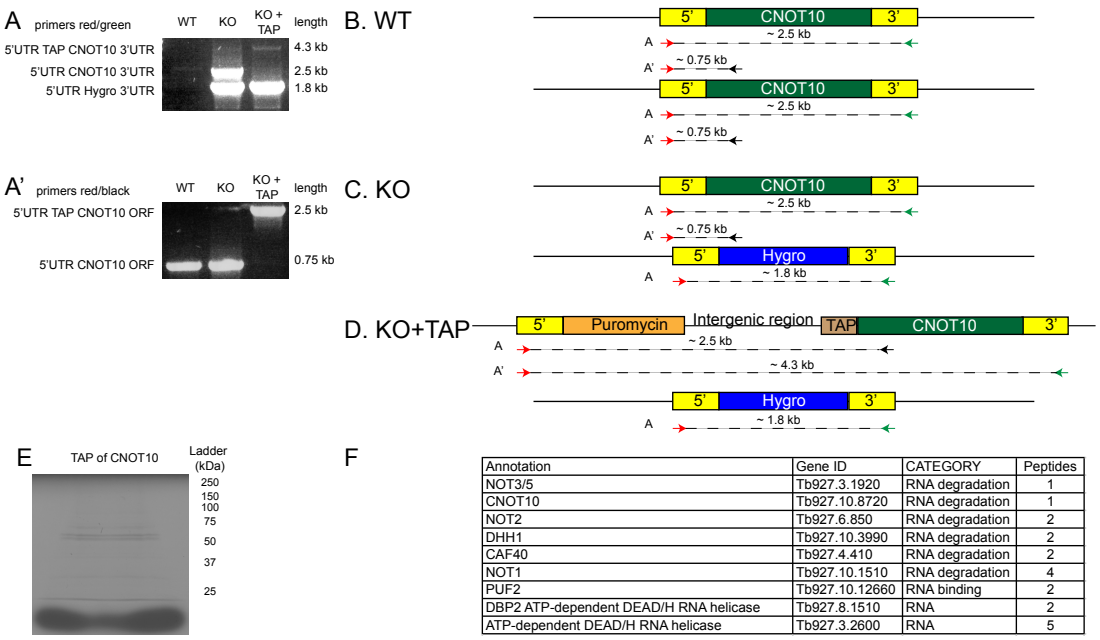

Annotation	Gene ID	CATEGORY	Peptides
NOT3/5	Tb927.3.1920	RNA degradation	1
CNOT10	Tb927.10.8720	RNA degradation	1
NOT2	Tb927.6.850	RNA degradation	2
DHH1	Tb927.10.3990	RNA degradation	2
CAF40	Tb927.4.410	RNA degradation	2
NOT1	Tb927.10.1510	RNA degradation	4
PUF2	Tb927.10.12660	RNA binding	2
DBP2 ATP-dependent DEAD/H RNA helicase	Tb927.8.1510	RNA	2
ATP-dependent DEAD/H RNA helicase	Tb927.3.2600	RNA	5

Figure 6 Tandem affinity purification of *Tb*CNOT10 in bloodstream form trypanosomes

(A) PCR primers annealing to the 5' and 3' UTR of *Tb*CNOT10 were used to verify the integration of the N-terminal TAP-tag and the knockout of wild-type *Tb*CNOT10. As expected, priming from the 5' and 3' UTR of *Tb*CNOT10 generated a 2.5 kb fragment in the wild-type cell line; compare with **(B)**. Two bands were visible in the single knockout cell line, one for the wild-type gene at 2.5 kb and a smaller one for the Hygromycin resistance at 1.8 kb; compare with **(C)**. Two bands were also seen for the TAP-tag CNOT10 cell line, one strong at 1.8 kb for the resistance marker (Hygro) and a second one, faint, for the *in situ* TAP-tagged *Tb*CNOT10 at 4.3 kb; compare with **(D)**. Differences in intensity are due to the PCR bias in favour of smaller fragments. **(A')** Priming from the 5'UTR of *Tb*CNOT10 and reverse from the middle of the ORF, one band was detected; compare with **(B, C and D)**. **(E)** shows a SDS-PAGE of the tandem affinity purification of *Tb*CNOT10, sent for mass spec. **(F)** shows an excerpt of the TAP results (the complete results can be found on the provided CD).

Although the peptide coverage was very low, I could identify all core members of the NOT complex in the mass spectrometry results, with the exception of CAF1 (Figure 6 F). This result is similar to a purification done in human cells by Lau et al. 2009, who were also unable to pull-down CNOT6/6L (CCR4) and 7 (CAF1a) using TAP-tagged *Hs*CNOT10. In contrast to an earlier performed TAP with CAF1 (38), I was able to observe the presence of CAF40. Additionally to the subunits of the complex, I could also purify two ATP-dependent DEAD/H RNA helicases, but these interactions could not be

verified due to a lack of antibodies. Another, ATP-dependent DEAD/H RNA helicase (*Tb*09.211.3510) was detected in the purification, but this helicase was already found several times in other TAP of our lab, which suggests that it is a rather common contamination due to its probable binding to the TAP-tag. Interestingly, I was able to identify one potential nuclear pore protein, encoded by *Tb*11.01.7010, which is a putative homologue of the yeast karyopherins Pse1p and Kap123p. An association of some members of the NOT complex with nuclear pore proteins was already shown in the human TAP by Lau et al. 2009, (67), but it is worth mentioning that no interaction between *Hs*CNOT10 and the nuclear pore proteins was identified. Furthermore, I could observe that the RNA-binding protein PUF2 was pulled down in the TAP, but co-immunoprecipitating PUF2 in a V5-tagged *Tb*CNOT10 BS cell line proved unsuccessful (Figure 7). A detailed list of all hits can be found in the attached CD.

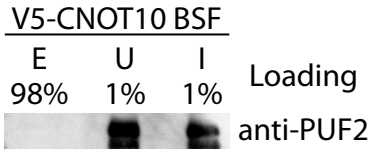

Figure 7 V5-CNOT10 does not interact with PUF2

$5x10^7$ trypanosomes expressing *in situ* V5-tagged *Tb*CNOT10 were used in a co-IP to detect a possible interaction of *Tb*CNOT10 and PUF2. (E=Eluate, U=unbound, I=input).

In this chapter, I could establish that *Tb*CNOT10 is a stable member of the CAF1-NOT complex in trypanosomes and that it might not interact with RNA binding proteins. In the following chapter, I attempt to show that members of the CAF1-NOT complex are essential for the growth of the parasite.

V.3. Most CAF1-NOT subunits are essential for the survival of trypanosomes

To see if *Tb*CNOT10 is essential for trypanosomes, I created permanent cell lines with inducible RNAi for the bloodstream and procyclic form of the parasite. RNAi was induced and after 36 hours, a severe proliferation defect could be observed in the bloodstream form of the parasite (Figure 8). In the slower growing procyclic form, it took about 60 hours to observe a decrease in cell numbers. At the same time, I also knocked down CAF16, CAF40, NOT2 and 3/5 in BS. For NOT3/5 and CAF40 a proliferation defect was observed (Figure 8 C, D) that was not visible for CAF16 and NOT2 (Figure 8 E, F). I could not verify the efficient knock down of *CAF16* since I did not detect any signal on the Northern blot. The rRNA might have masked the mRNA signal because it was at the same place. However, I did not follow up this result as sequence analysis of the putative CAF16 indicated that it is not a homologue of CAF16 in other eukaryotes, but a putative ABC transporter (TriTrypDB *Tb*927.6.2810). In the case of NOT2, the RNAi was not very efficient in all tested clones. A high-throughput RNAi screen done by Alsford et al. in 2011 (161) yielded the same results, that is say, no RNAi effect could be detected. To verify that an RNAi efficiently reduced the protein level of *Tb*CNOT10, I created a cell line harbouring a N-terminal *in situ* V5-tagged *Tb*CNOT10, in addition to its inducible RNAi targeting *Tb*CNOT10. Upon tetracycline induction, the protein level of V5-tagged *Tb*CNOT10 decreased after one day (Figure 8 G).

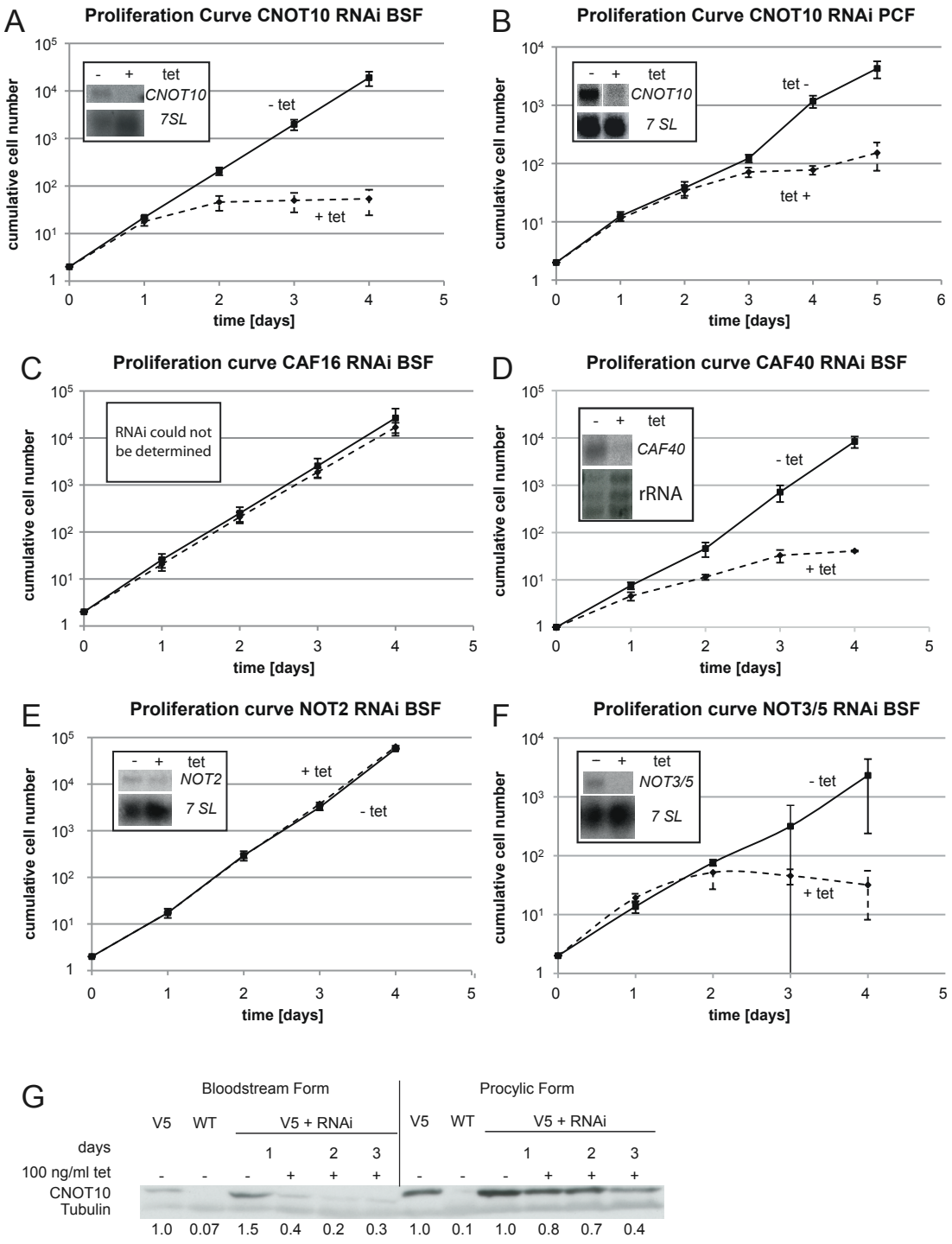

Figure 8 RNAi screen targeting several subunits of the CAF1-NOT complex in *T. brucei*

An RNAi screen was performed against all canonical (CAF40 and NOT2, 3/5) and potential (CAF16 and *Tb*CNOT10) subunits of the CAF1-NOT complex in *T. brucei* (**A-F**). In the bloodstream form of the parasite, the proliferation experiment was conducted over a period of four days and in the procyclic form five days. (**G**) The protein amount of *Tb*CNOT10 decreased after one day of tetracycline induction, in both life stages of the parasite.

Through my experiments, I could show that *Tb*CNOT10 is essential for the proliferation of the parasite in both life stages. Interestingly, this was also the case for NOT3/5 and CAF40. My decision to focus on *Tb*CNOT10 relies on the fact that it differs a lot from its orthologues in other eukaryotes and is both a stable and an essential member of the complex.

V.4. Purification of recombinant *Tb*CNOT10

In order to raise an antibody and conduct enzymatic assays, *Tb*CNOT10 was N-terminal His-tagged and expressed in the *E. coli* strain BL21. The expression was induced by the addition of 0.1 mM IPTG two hours prior harvesting. His-tagged *Tb*CNOT10 was not soluble under various conditions (e.g. different *E. coli* strains, cell densities, concentrations of IPTG, growth under various temperatures) and hence eluted under denaturing conditions, using the denaturing elution buffer supplemented with 300 mM Imidazole. The efficiency of the purification was very low and contained a lot of undesired protein contaminations beside the His-tagged *Tb*CNOT10. Although high stringent elution conditions were applied, most of the recombinant protein remained bound to the beads. Figure 9 shows a representative purification attempt of His-tagged *Tb*CNOT10. An attempt to express soluble *Tb*CNOT10 by using another plasmid system failed. This plasmid (pET-Trx, gift from AG Krauth-Siegel) encodes for a thioredoxin fusion protein, which is supposed to enhance the solubility of the expressed recombinant protein. Unfortunately, I was not able to see the expression of *Tb*CNOT10 after the induction of IPTG.

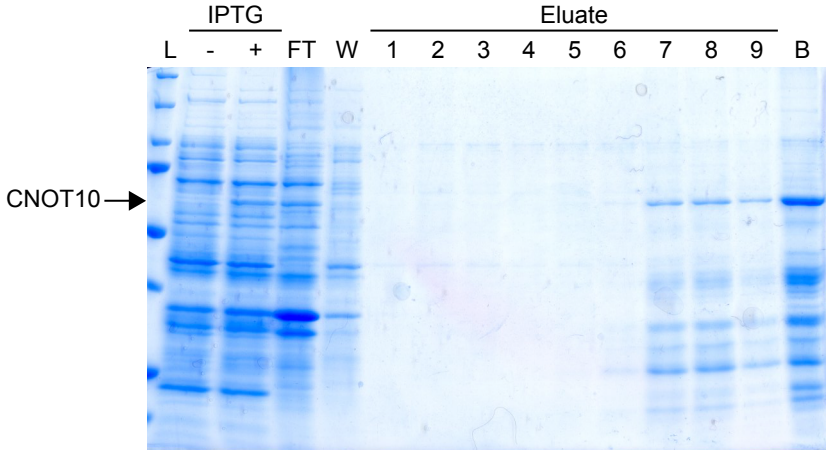

Figure 9 His-tagged *Tb*CNOT10 purification

His-tagged *Tb*CNOT10 was purified under denaturing conditions from His-beads using an elution buffer containing an additional 300 mM Imidazole at pH 4.5. The protein was retrieved from the beads with a lot of contaminations (L=Ladder, FT=Flow through, W=Wash I-IV, B=Beads).

Considering the functionality and good expression of V5- and/or TAP-tagged *Tb*CNOT10, I decided to use them for all future experiments and stop with protein purification.

V.5. *Tb*CNOT10 is located in the cytoplasm

In immunofluorescence microscopy, TAP-tagged *Tb*CNOT10 was detected in a rather granular pattern in the cytoplasm (Figure 10).

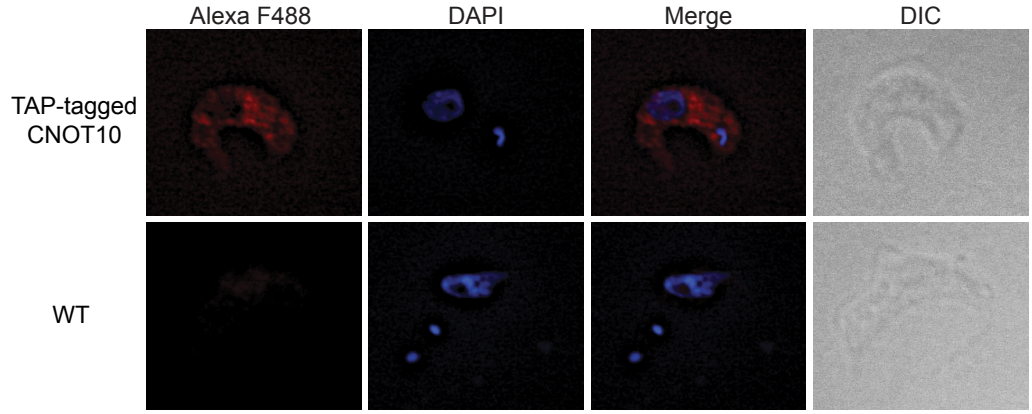

Figure 10 Immunofluorescence of N-terminal *in situ* TAP-tagged *Tb*CNOT10

TAP-tagged *Tb*CNOT10 was detected by immunofluorescence. DAPI indicates the position of the Nucleus and Kinetoplast. Differential interference contrast (DIC) microscopy shows the parasite's cell body.

V.6. *Tb*CNOT10 is essential for proper mRNA turnover

My next step was to analyse the effect of *Tb*CNOT10 depletion on mRNA degradation. Three mRNAs (actin (*ACT*), histone H4 (*HISH4*) and EP procyclin (*EP*)) were analysed and in general, mRNA degradation was inhibited with chemical inhibitors (Figure 11 A, B, C). In *Tb*CNOT10-depleted cells, the half-life of actin mRNA (*ACT*) was delayed by around 30 min and deadenylation was reduced as could be verified in the slower decrease of the bands' size in comparison to wild-type. Moreover, the steady-state level of *ACT* increased 5.7-fold after *Tb*CNOT10 depletion (Figure 11 A). When I looked at the mRNA of Histone H4 (*HISH4*), I could also observe an increase of its half-life, but both steady-state and deadenylation seemed to be unaffected (Figure 11 B). The half-life of *EP* was strongly deferred by over 90 min, deadenylation reduced and the steady-state raised 3.5-fold (Figure 11 C) (58). These results are comparable to a knockdown of *CAF1*, although *HISH4* deadenylation was inhibited in CAF1-depleted cells (38).

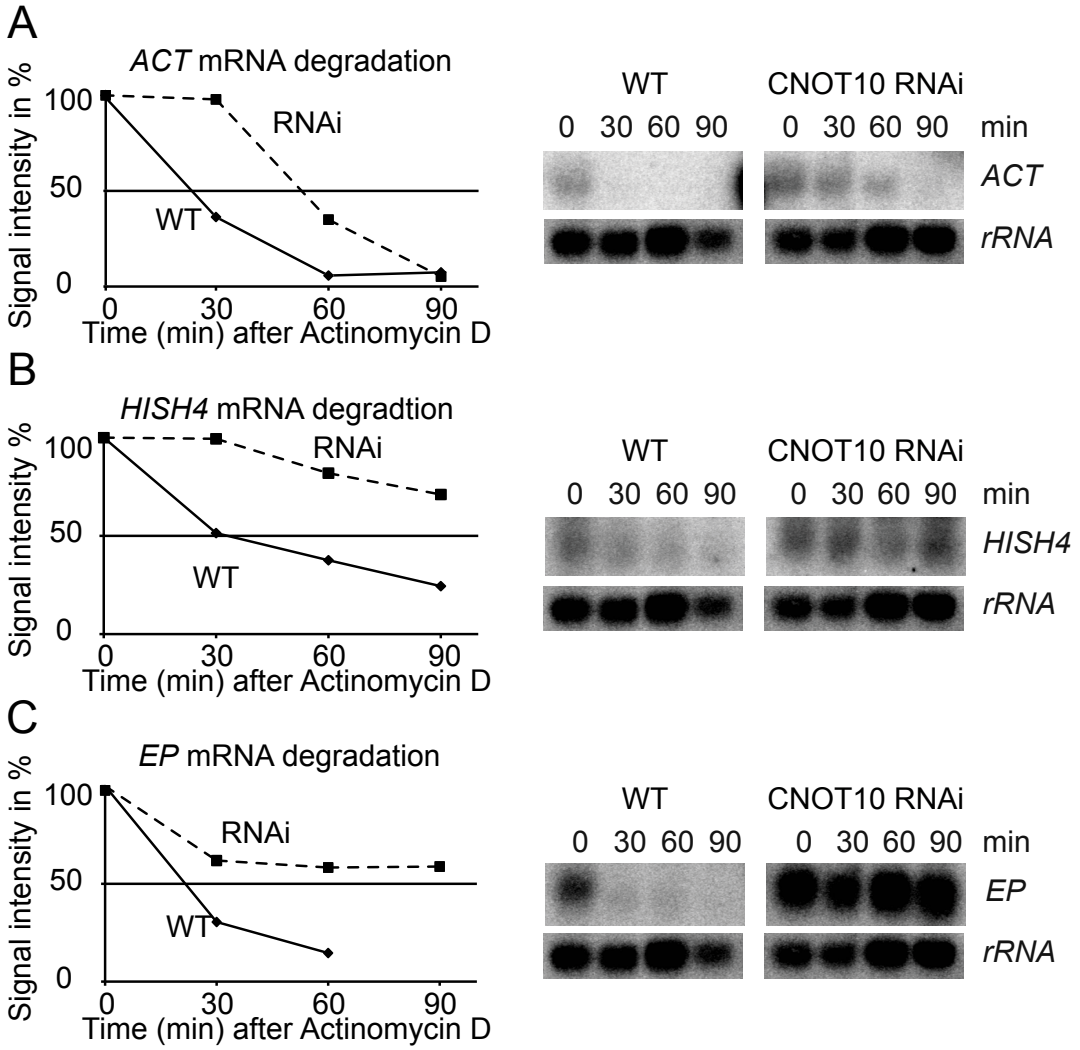

Figure 11 mRNA degradation assay upon *Tb*CNOT10 depletion

*Tb*CNOT10 was depleted for 36 h by RNAi in *T. brucei*. Then, transcription was inhibited by the addition of chemical inhibitors (Sinefungin, Actinomycin D) and followed by the collection of cells at 0, 30, 60 and 90 min. In **(A, B, C)** Northern Blots of mRNA degradation assays, analysing the degradation of *ACT*, *HISH4* and *EP*, are shown for wild-type and *Tb*CNOT10 depleted cells. The obtained signals were normalised to rRNA. **(A)** The signal for *ACT* (each n=6) was quantified for wild-type and *Tb*CNOT10 RNAi and results were plotted as mean. The dashed line and square box represent RNAi whereas diamonds and continuous line represent wild-type. The same was done for *HISH4* (n=4) **(B)** and for *EP* (n=6) **(C)**. In **(C)**, the last time point for WT is not shown due to the degradation of *EP*.

To assess if *Tb*CNOT10 depletion influences only certain mRNAs or rather acts globally, I repeated the mRNA degradation assays. The isolated RNA, depleted of rRNA, was sent to the Deep Sequencing facility of the Bioquant for RNAseq. Additionally, I sequenced mRNA degradation assays

for *CAF1*-, PAN2- and RRP45-depleted cells. The RNAi efficiency was verified by Northern blots (Figure 12 A-D).

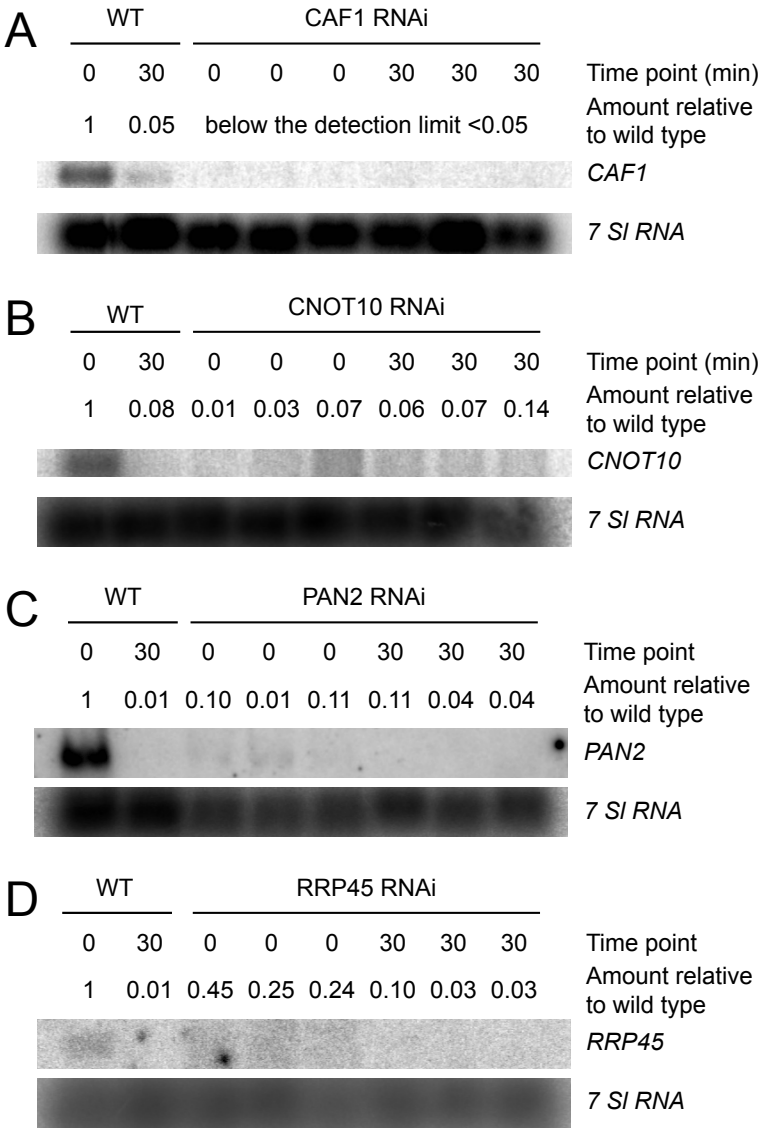

Figure 12 RNAi verification of the analysed knockdown cell lines

RNA samples were taken at each time point in order to assess the efficiency of the knockout. **(A-D)** show the Northern blots for each experiment. The Signal was normalised to 7 SL RNA.

To normalise the received results for differences in e.g. RNA amounts and library preparation efficiency, I ran Northern blots with an aliquot of each sample and hybridised them with a radioactive labelled spliced leader oligo, as shown in Figure 13 A-E. In wild-type cells, 54 % of the total mRNA was left after 30 min of transcription inhibition (Figure 13 A). When I depleted the cells of CAF1, *Tb*CNOT10 and RRP45 I could observe a stronger signal for bulk

mRNA, meaning that overall mRNAs became more stable. Knocking down PAN2 had only a minor effect (Figure 13 D).

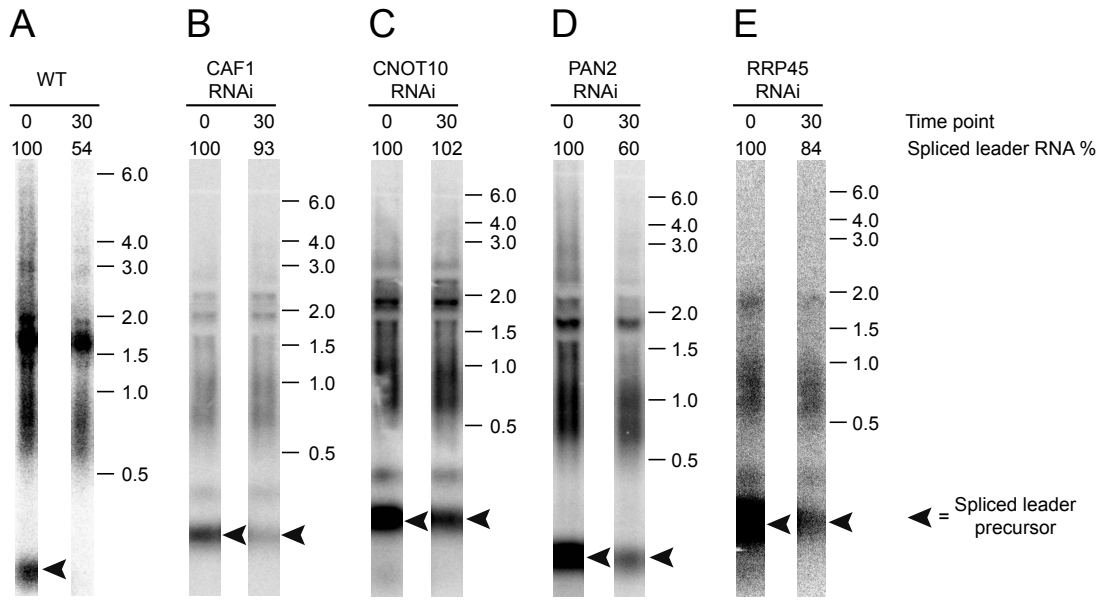

Figure 13 Spliced leader control for RNAseq samples

An aliquot of each sample was loaded on a 1.5 % RNA-gel to determine the overall mRNA half-life. **(A)** shows the signal from the spliced leader at time point 0 and 30 min from wild-type cells. Figures **(B-E)** show the signal from the spliced leader for time point 0 and 30 min for the knockdown cell lines CAF1, *Tb*CNOT10, PAN2 and RRP45.

The normalised RNAseq data showed that knocking down *Tb*CNOT10 led to a halt in mRNA degradation and increased the half-life of most mRNAs to over 60 min. The same result was obtained in CAF1- and RRP45-depleted cells, but RNAi targeting PAN2 had only a minor effect on the stability of mRNAs (Figure 14 - Abeer Fadda undertook all related bioinformatic and statistical analyses).

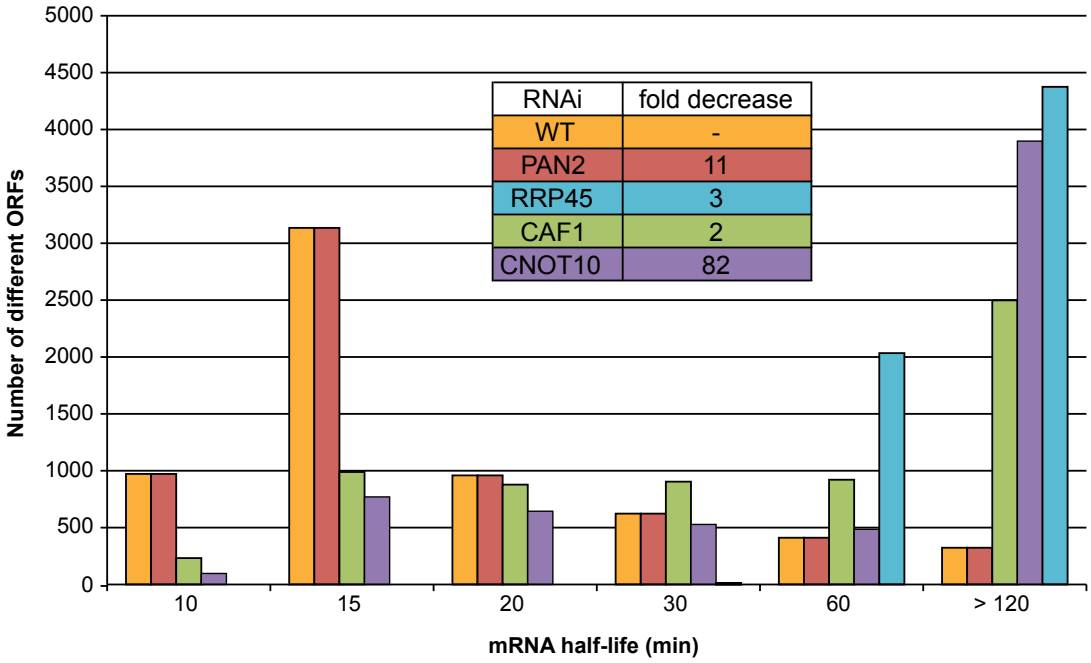

Figure 14 Overview of mRNA half-lives after RNAi

The diagram shows the number of different open reading frames (ORFs) and their corresponding mRNA half-life. mRNAs from wild-type cells are coloured in orange, PAN2-depleted cells in red, RRP45-depleted cells in blue, CAF1-deplted cells in green and CNOT10-depleted cells in purple. The box illustrates the efficiency of the RNAi, using the corresponding sequence reads of the knockdown and comparing them to WT.

These results indicate that *Tb*CNOT10 is important for proper deadenylation and mRNA degradation in *T. brucei*. As expected, CAF1 is essential for normal mRNA degradation, whereas PAN2 has no effect. Surprisingly, a knockdown of RRP45 inhibited mRNA degradation in the same way as an inhibition of deadenylation (Depletion of CAF1 and *Tb*CNOT10) did. My next steps attempt to understand the role of *Tb*CNOT10 in mRNA turnover.

V.7. *Tb*CNOT10 is essential for the interaction of CAF1 with the major deadenylase complex

To find out whether *Tb*CNOT10 is necessary for the stability of the complex, I used glycerol gradient centrifugation to analyse it. For these experiments, I used mixtures of cell lysates from trypanosomes expressing V5-tagged versions of CAF1, NOT1 or cells expressing V5-tagged CAF1

depleted of *Tb*CNOT10. CAF1, *Tb*CNOT10 and NOT1 all migrated between fractions 9 to 20, with the major peak of the CAF1-NOT complex in fractions 13 – 18. In addition, a major part of CAF1 was in the lighter fractions 2 – 8 and hence not associated with the complex. When I knocked down *Tb*CNOT10 by RNAi, CAF1 no longer co-migrated with the complex (Figure 15 B). Quantification of 3 independent gradients clearly confirmed that CAF1 was no longer associated with NOT1 after *Tb*CNOT10 depletion (Figure 15 C and D).

This result suggests that *Tb*CNOT10 is essential for the interaction of CAF1 with the rest of the NOT complex.

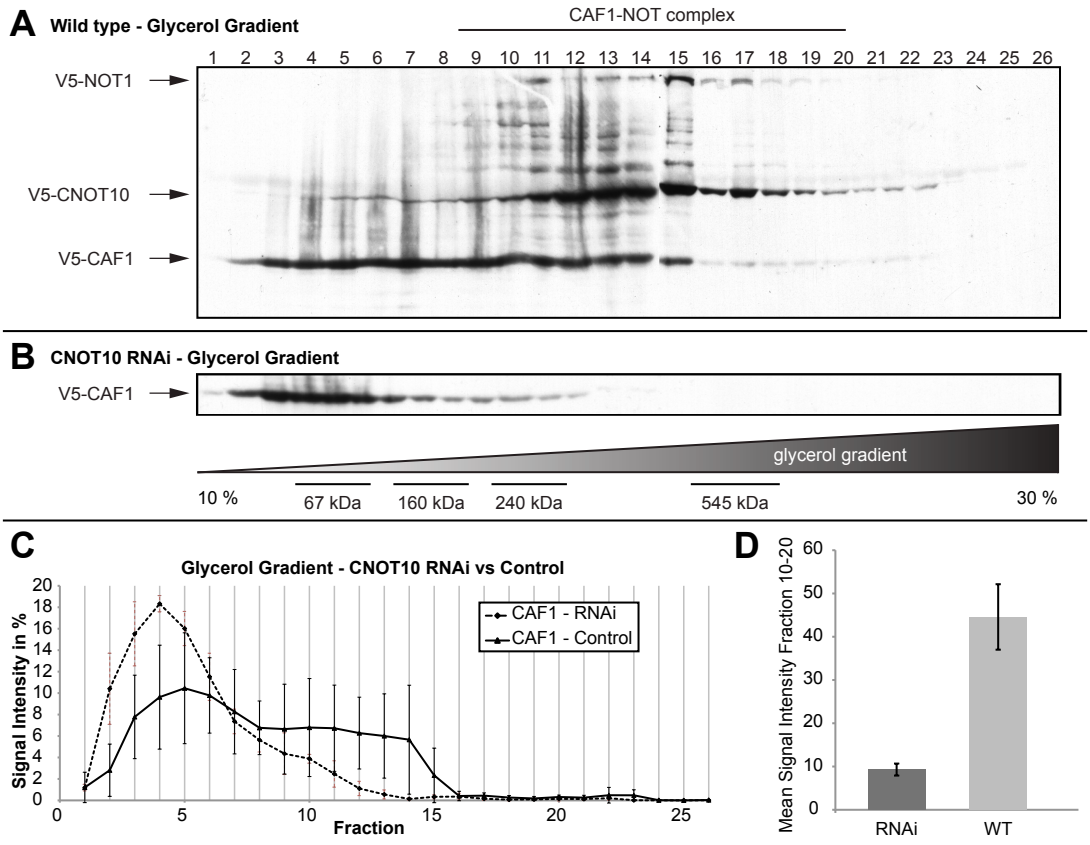

Figure 15 Glycerol Gradient of the CAF1-NOT complex of *T. brucei*

(A) The extract of three different cell lines (*in situ* V5-tagged CAF1, *Tb*CNOT10 and NOT1) were mixed and run on a 10 – 30 % Glycerol Gradient. The gradient was divided into 26 fractions. The size indications are shown at the bottom of Figure **(B)**. Figure **(B)** presents a Glycerol gradient of *Tb*CNOT10-depleted cells and in situ V5-tagged CAF1. **(C)** shows the quantification of the signal of 3 independent gradients in percent (total mean signal) of V5-CAF1 in *Tb*CNOT10-depleted cells (dashed line; n=3) and control (black line; n=3). A comparison of the V5-CAF1 Western blot signal from fraction 10 – 20 is shown in **(D)**.

V.8. *Tb*CNOT10 depletion reduces the amount of NOT1

To define the interactions within the *Trypanosoma* CAF1-NOT complex in more detail, Esteban Erben analysed them using the yeast two-hybrid system. Due to the large size of NOT1, we decided to analyse the N- and C-terminal portions separately. The experiments showed that *Tb*CNOT10 directly interacted with CAF1, NOT5 and with the N- and C-terminal part of NOT1 (Figure 16). The interaction between *Tb*CNOT10 and NOT3/5 could be shown only with *Tb*CNOT10 as the prey and NOT3/5 as the bait. CAF1 interacted with *Tb*CNOT10 and the N-terminal part of NOT1, but not with NOT3/5. The interactions of CAF1 with the C-terminal part of NOT1 were shown only in one direction and only under low stringency conditions.

AD → / BD ↓	CAF1	CNOT10	NOT1-Nt	NOT1-Ct	NOT3/5	T7
CAF1	+++	+++	+++	+	-	-
CNOT10	+++	+++	+	+	-	-
NOT1-Nt	+++	+++	+	-	-	-
NOT1-Ct	-	+++	-	-	-	-
NOT3/5	-	+++	-	-	-	-
Lamin	-	-	-	-	-	-

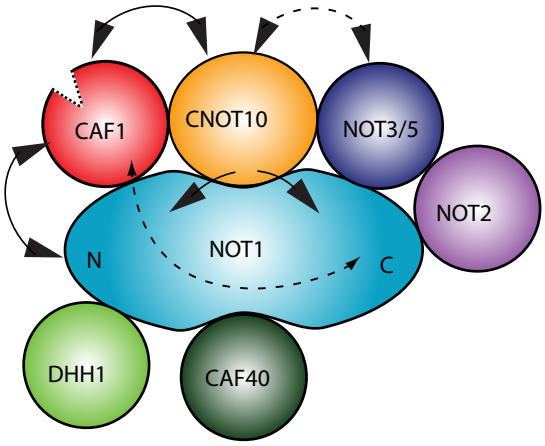

Figure 16 Yeast two-hybrid interactions in the CAF1-NOT complex

Left: Minus and plus signs indicate the absence or presence of interaction detected by the activation of the *His3* and *LacZ* reporters; multiple pluses indicate the activation of the *Ade2, His3* and *LacZ* reporters. Lamin and T antigen (7) are negative controls. **Right:** Illustration of the CAF1-NOT complex. Lines indicate interactions between different subunits; a dashed line means that the interaction could be proved in only one direction.

To analyse whether *Tb*CNOT10 depletion directly affects the amount of CAF1 or NOT1, I knocked down *Tb*CNOT10 in cells expressing V5-CAF1 or V5-NOT1 over a period of 2 days and analysed protein levels by Western blot.

V5-CAF1 was not influenced by a depletion of *Tb*CNOT10 (Figure 17 A, lane e.g. 3 and 4), but NOT1 was decreased (Figure 17 B, lane e.g. 3 and 4).

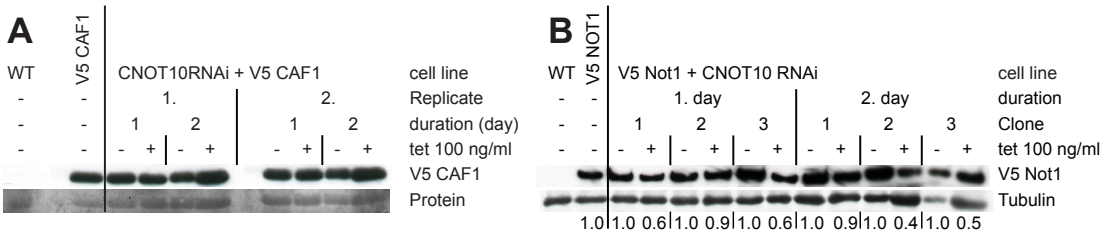

Figure 17 *Tb*CNOT10 knock down leads to decrease of NOT1

(A) The level of *in situ* V5-tagged CAF1 was measured after *Tb*CNOT10 depletion over a period of 2 days. **(B)** The effect of *Tb*CNOT10 RNAi on *in situ* V5-tagged NOT1 was analysed in three different clones over a period of 2 days.

To confirm the results, I analysed the interactions by co-immunoprecipitation in cells with normal amount of *Tb*CNOT10 and in *Tb*CNOT10-depleted cells. First, I tried to determine if CAF1-myc and V5-CAF40 could pull each other down. In cells with normal amounts of *Tb*CNOT10, precipitation of CAF1-myc resulted in coprecipitation of V5-CAF40 (Figure 18 A lane 6), but this no longer occurred in cells depleted of *Tb*CNOT10 (Figure 18 A lane 9). The results were confirmed by reciprocal pull-down (Figure 18 B lane 6 and 9). I further analysed the association of CAF1 and NOT1 by co-IP, to see if the interaction is *Tb*CNOT10-dependent. In V5-NOT1 and inducible CAF1-myc cells, a pull-down of CAF1-myc yielded V5-NOT1 as interaction partner (Figure 18 C lane 6), but CAF1-myc could not coprecipitate NOT1 in CNOT10-depleted cells (Figure 18 C lane 9). In cells with normal levels of *Tb*CNOT10, co-IP of V5-tagged NOT1 resulted in CAF1-myc pull-down (Figure 18 D lane 6). However, when I knocked down *Tb*CNOT10 and V5-NOT1 was pulled down, there was only a slight reduction of the interaction between CAF1 and NOT1 (Figure 18 D 9). So far, I was unable to account for this discrepancy but my hypothesis is that all remaining NOT1 is the fraction that is bound to CAF1.

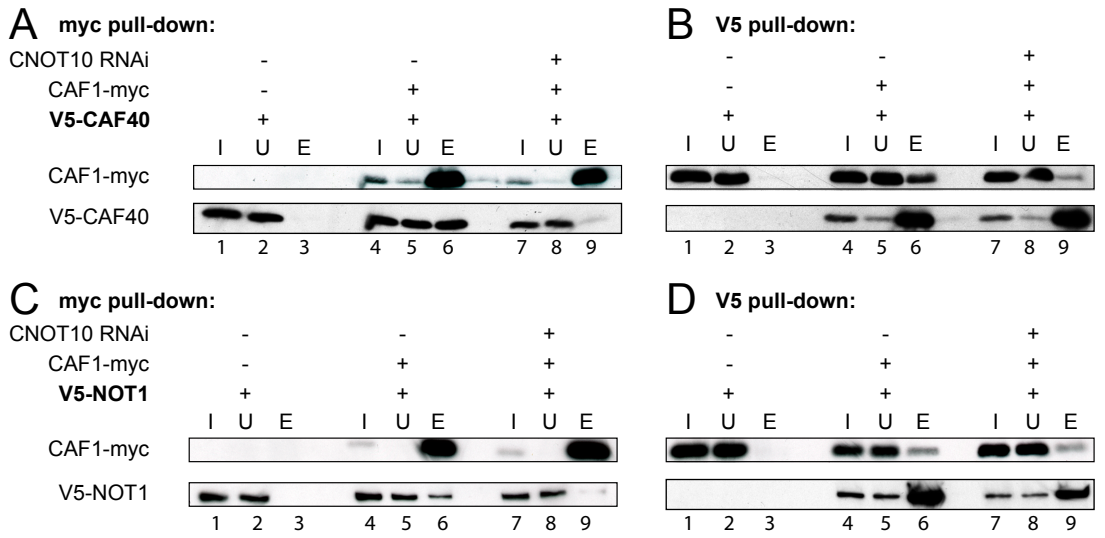

Figure 18 Depletion of *Tb*CNOT10 reduces CAF1 association with the complex

1% was loaded for input (I) and supernatant (S) and the rest was eluted (E). **(A)** anti myc-beads were used to pull-down myc-tagged CAF1 in wild-type cells (lanes 4-6) and cells with *Tb*CNOT10 RNAi (lanes 7-9). Cells expressing V5-tagged CAF40 alone (lanes 1-3), without myc-tagged CAF1, were used as a negative control. Figure **(B)** shows the reciprocal experiment using V5-beads. **(C, D)** as in **(A, B)** respectively, but here the interaction between CAF1 and NOT1 was analysed with or without *Tb*CNOT10 RNAi.

The yeast two-hybrid experiments showed that both CAF1 and *Tb*CNOT10 directly interact with NOT1. Moreover, *Tb*CNOT10 is probably important for the stability of NOT1, and for the interaction between CAF1 and NOT1.

V.9. CAF1 deadenylation activity is not complex-dependent

My results so far suggested that in vivo, when CAF1 is not in the NOT complex, CAF1 is unable to initiate mRNA degradation. However, our lab had previously shown that recombinant CAF1 is active in deadenylation in vitro (38). There are two possible explanations for this discrepancy. Either CAF1 enzyme activity *in vivo* might be complex-dependent, or CAF1 relies on the complex for attachment to substrates. To distinguish these possibilities, I used a cell line containing a constitutively-expressed mRNA reporter that consisted of a *GFP* ORF followed by six boxB elements and an actin 3'UTR. In addition, the cell line inducibly expressed a CAF1 fusion protein with a λN peptide at the N-terminus and myc at the C-terminus (λN-CAF1-myc). As expected, upon induction of λN-CAF1-myc expression, *GFP*-boxB mRNA was destroyed (Figure 19, lane 1, 2 and 7, 8). Control RNA with no boxB was unaffected by λN-CAF1-myc expression (not shown). However, I cannot exclude that in the experiment, tethered CAF1 might still interact with the NOT complex. Therefore, I depleted *Tb*CNOT10 by RNAi in order to eliminate the interaction and thus, CAF1 alone should be tethered. Nevertheless, tethered CAF1 still induced the degradation of the *GFP*-boxB mRNA reporter (Figure 19, lane 3,4 and 5,6 as well as 9,10 and 11,12). This suggests that CAF1 alone is indeed active *in vivo* (as expected from *in vitro* activity), but that it depends on the presence of *Tb*CNOT10 to be recruited to its substrate. However, RNAi is never 100 % efficient and hence *Tb*CNOT10 might not be depleted sufficiently to stop degradation.

The results indicate that *Tb*CNOT10 is essential for the recruitment of CAF1 to mRNAs, but is not responsible for it.

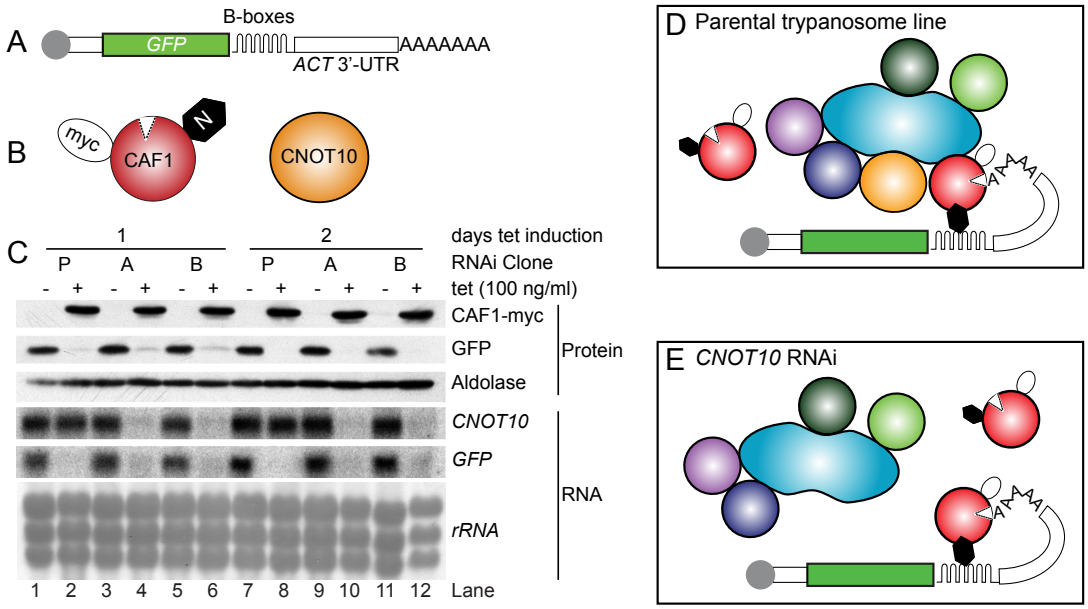

Figure 19 Tethering CAF1 to a *GFP* reporter mRNA

(A) The illustration shows the reporter mRNA used in this experiment. The cap structure of the mRNA is indicated in grey and the *GFP* ORF in green. A 6 B-box loops resides at the start of the *ACT* 3'UTR. **(B)** λN-CAF1 myc-tagged is shown in red and *Tb*CNOT10 in orange. **(C)** shows Western and Northern blots of GFP protein (above) and *GFP* mRNA. The Western blots also show the inducible expression of λN-CAF1-myc as well as Aldolase control. In the Northern blots below, *TbCNOT10* mRNA is shown and rRNA was used as a loading control. **(D)** In the parental cell line ((C) P – lane 1,2,7,8) λN-CAF1-myc is tethered to the *GFP* reporter mRNA, upon tetracycline induction due to their interaction through the λN peptide and the 6 B-box loops respectively. λN-CAF1-myc interacts with the NOT complex and is able to degrade the reporter. **(E)** In cell line A and B, *Tb*CNOT10 is diminished upon RNAi for 1 ((C) lane 4,6) and 2 days ((C) lane 10,12). *CAF1* is still tethered to the reporter RNA and can still degrade poly(A), even though association with the NOT complex has decreased. (Parts of this figure were prepared by Prof. CE Clayton)

V.10. *Hs*CNOT10 is not required for the association of CAF1 with the major deadenylation complex

Given the importance of *Tb*CNOT10 in mRNA degradation, I became interested in finding out if its function was conserved in mammalian cells. Therefore, I collaborated with Sahil Sharma from the Stoecklin Group of the DKFZ, who first confirmed the interaction of *Hs*CAF1a and *Hs*CNOT10 in human embryonic kidney (HEK) 293 cells by co-immunoprecipitation (Figure 20 A). Using myc-strep-tagged *Hs*CAF1a, he was able to pull-down *Hs*CNOT10 and could confirm the interaction previously shown by tandem affinity purification (162). To find out whether the association of *Hs*CAF1a with the human CCR4-CAF1-NOT complex is CNOT10-dependent, he knocked down *Hs*CNOT10 by siRNA and used a scrambled siRNA as well as a siRNA targeting *Hs*NOT1 as controls. Together, we analysed the migration of *Hs*CAF1a in a glycerol gradient. Figure 20 B shows that *Hs*CNOT10 depletion did not influence the migration of *Hs*CAF1a, while a knockdown of *Hs*NOT1 led to a shift of *Hs*CAF1a towards lighter fractions. The knockdown efficiency of *Hs*CNOT10 and *Hs*NOT1 was verified by Western Blot analysis (Figure 20 C).

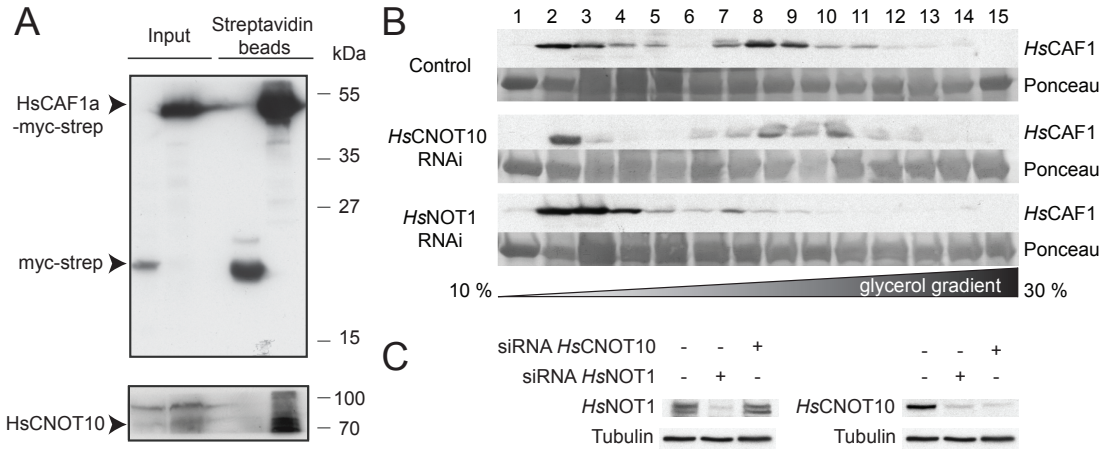

Figure 20 Co-immunoprecipitation of HsCAF1 and HsCNOT10 and glycerol gradients of HsCAF1

(A) Using myc-strep-tagged *Hs*CAF1a, we were able to pull-down *Hs*CNOT10 in HEK cells. **(B)** Control, human CNOT10 and NOT1 RNAi extracts were run on a 10 – 30 % glycerol gradient and 15 fractions were collected. The Western blots of the gradients were analysed for the migration of *Hs*CAF1a. Knock down of *Hs*CNOT10 did not affect the migration of *Hs*CAF1a, but a knock down of HsNOT1. **(C)** The knock down efficiency for *Hs*NOT1 and *Hs*CNOT10 was verified by Western blots.

The results suggest that *Hs*CNOT10 is not required for association of *Hs*CAF1 with *Hs*NOT1 in mammalian cells.

VI. Discussion

The CAF1-NOT complex is responsible for most deadenylation in *T. brucei*. In a previous study conducted in our lab, CAF1 was identified as the major deadenylase in trypanosomes (38), and it is known that NOT1 acts as the major scaffold of the complex (76, 163). The aim of my PhD was to identify the essential subunits of the complex and their subsequent characterization. My decision to characterise *Tb*CNOT10 was based on the fact that this subunit is essential for proliferation of the parasite and differs greatly from its orthologues in other eukaryotes.

VI.1. CNOT10 is an essential cytoplasmic subunit of the CAF1-NOT complex in trypanosomes

A tandem affinity purification of CAF1 revealed known (NOT1, NOT2, NOT3/5, DHH1) and putative (CNOT10-like protein, CAF16) subunits of the CAF1-NOT complex in trypanosomes (38). Several *in silico* results confirmed that *Tb*927.10.8720 is an orthologue of CNOT10. Moreover, *Tb*CNOT10 has a Tetratrico peptide repeat (TPR)-like domain comparable to its counterpart in other eukaryotes. The retrieved e-values (below 3e-04 to 1e-07) to potential orthologues were good and a reciprocal blast search of CNOT10 in human and trypanosome always showed CNOT10 as the first hit. Beside the *in silico* data, the co-IP of CAF1 and CNOT10 confirmed that it is a stable member of the CAF1-NOT complex. The fact, that CAF1 could only partially pull-down CNOT10 (and vice versa) is no surprise. Indeed, the results of the glycerol gradient experiments showed that around 50 % of CAF1 was not bound to the NOT complex in trypanosomes. Moreover, N-terminal protein-A-calmodulin-binding-peptide tag CNOT10 could pull-down all core subunits of the CAF1-NOT complex, except CAF1. This is not surprising considering the amount of unbound CAF1 in the cell. In a TAP of *Hs*CNOT10 bearing a N-terminal FLAG-HA tag, the same results were obtained (67). In this study, CAF1a could be pulled down by CNOT2, CNOT3, CNOT6 (CCR4) and CNOT9 (CAF40). Our glycerol gradients in HEK cells also indicate that a fraction of human CAF1a is not bound to the complex even though glycerol gradients

with HeLa cells gave a different result (79). The discrepancy between the cell lines might be explained by fact that the human CCR4-CAF1-NOT complex seems to exhibit a tissue-specific expression pattern (69, 88).

The immunofluorescence microscopy experiments showed that TAP-tagged *Tb*CNOT10 reside in the cytoplasm like other subunits of the complex (38). However, the TAP-tag (N-terminal protein-A-calmodulin-binding-peptide) prevented colocalisation experiments to further analyse the rather granular pattern and the signal for V5-tagged CNOT10 was below the detection limit. To solve this issue, one could conduct further experiments with other tags (myc-tag or GFP fusion protein) or raise an antibody. The tags can never represent the native state of the protein in the cell and hence it is necessary to continue the efforts in raising an antibody against *Tb*CNOT10 in order to further characterise its location. None of the efforts in purifying a recombinant protein led to a satisfactory expression. Moreover, after stringent washing conditions under denaturing conditions, N-terminal His-tagged CNOT10 remained on the column. This behaviour could be on account of the TPR–like domain, which is known to be involved in protein-protein interaction (164) and hence might be responsible for the increased adherence to the resin. Thus, cloning only a N-terminal fragment of *Tb*CNOT10 lacking the TPR-domain could be a possible solution. To overcome the solubility issue, I have tried several recommended actions, e.g. expression at different temperatures, cell density, using different plasmids (pET-Trx), etc., but none of these attempts proved successful. However, one could try to increase the solubility by adding charged amino acids (L-Arg and L-Glu) as recommended by Golovanov et al. in 2004 (165). I decided to work with only the tagged-versions (V5 or TAP) of CNOT10, because the purification of the recombinant protein demanded too much time and, more importantly, I could show that the tagged *Tb*CNOT10 (V5 or TAP) were functional, by deleting the remaining wild-type copy.

The RNAi screen against subunits of the CAF1-NOT complex (CAF16, CAF40, CNOT10, NOT2, NOT3/5) revealed that almost all investigated proteins are essential for the growth of the parasite except for the CAF16-like protein and NOT2. In regards to the putative CAF16, I did not observe any signal on the Northern blot and hence could not confirm the efficacy of the knockdown. The signal might have been masked by the rRNA signal, which

runs at the same place on the Northern blot. A poly(A) tail purification of the total RNA might have led to an enrichment of the signal, but *in silico* studies revealed that the gene locus *Tb*927.6.2810 encodes for a putative ABC transporter and not for CAF16 so I did not proceed. For NOT2, the RNAi efficiency was very low in all studied clones. Nevertheless, a RNAi screen by Alsford et al. in 2011 also showed no growth defect for *Tb*927.6.2810 (putative ABC transporter) and NOT2 (161).

VI.2. The role of exoribonucleases and *Tb*CNOT10 in mRNA turnover

Depletion of *Tb*CNOT10 led to an increase of the steady-state levels of *EP* and *ACT*, two unstable mRNAs, but not that of *HISH4*. This is comparable to a knockdown of CAF1 although its depletion only led to an increase of the steady-state level from *EP* (38, 58). The elevation of *ACT*'s steady-state triggers new questions. In yeast, it was indicated that steady-state levels of RNAs transcribed by RNA Pol II remain stable due to a feedback response (166). In *S. cerevisiae*, Rpb4p and Rpb7p, two subunits of RNA Pol II, were shown to shuttle mRNAs out of the nucleus by binding to them. Once in the cytoplasm, Rpb4/7p stimulates degradation of the bound RNAs by inducing deadenylation and recruiting the Pat1/Lsm1-7 complex (167, 168). A recent genome-wide transcriptome study in yeast, that used a mutant of Pol II leading to a poor recruitment of Rpb4/7p, proposed an explanation to the mechanism behind the feedback loop. They suggested that the proportion of Rpb4/7p-bound mRNAs and unbound mRNAs may change depending on the situation of the cell (166). In the case of CAF1-depleted trypanosomes, this would mean that the amount of transcripts that are shuttled out by Rpb4/7 increases. However, this no longer holds true when *Tb*CNOT10 is depleted. In this case, it seems that either Rpb4/7 depends on *Tb*CNOT10 to stable associate with certain transcripts or Rpb4/7-coated transcripts are simply not degraded in the absence of *Tb*CNOT10. In both case, the lack of *Tb*CNOT10 allows the steady-state level of some transcripts to increase.

The genome of *T. brucei* possesses putative homologues of Rpb4 (Tb927.3.5270) and Rpb7 (Tb11.01.6090) and the role of these subunits in transcriptions is still under discussion (169-173). In addition, the RNAi screen by Alsford showed that they are only essential in the bloodstream form (161), which indicates either that these subunits do not contribute to a general feedback loop in *T. brucei* or that this feedback loop is only present in the bloodstream form of the parasite. However, *Tb*CNOT10 was depleted in bloodstream cells and the steady-state levels still rose, which implicates that there must be different feedback mechanisms involved in the regulation of the steady-level of mRNA transcripts. For example, mRNA transcription might depend on the ribonucleotides provided by mRNA decay and thus, once mRNA decay stops, the steady-state level remains unchanged because no further transcripts can be provided due to a lack of ribonucleotides. This might also explain why only some RNAs show increased steady-state levels. Indeed, mRNA turnover did not completely stop in the RNAi mutants, thus permitting transcription to continue since ribonucleotides were still provided by mRNA decay. Therefore, it would be interesting to further study the effect of the knockdown mutants on steady-state.

In the case of *EP* in particular, it was clear that deadenylation was slowed down in CNOT10-depleted cells because full-length mRNAs were still visible even after 90 min. The bulk mRNA turnover experiments (Northern blots with spliced leader and RNAseq) showed that *Tb*CNOT10 depletion leads to a halt in mRNA degradation, similar to a knock down of CAF1 and RRP45. The less efficient RNAi of CAF1 might explain the differences between CAF1 and CNOT10. PAN2 depletion did not have an effect on bulk mRNA turnover, indicating that the CAF1-NOT complex might be able to compensate its lack. The observation that the PAN2-PAN3 complex is not essential in yeast and got lost in many organisms during evolution (58) also indicates that its function can be replaced. The major effect of RRP45 knockdown was rather surprising because one can suspect that not all mRNAs are degraded through the 3'->5' degradation pathway (8, 58). Previous studies have shown that in *T. brucei*, mRNA degradation can occur from both ends, that is to say either by XRNA or the exosome (58, 147). The evidence for this was based on the

observation that an *EP* RNA reporter showed polyadenylated degradation products and that degradation was inhibited in XRNA-depleted cells (58). In the same study, deadenylated *EP* reporter RNA intermediates could also be detected, thus proving the existence of a 3' – 5' degradation pathway. The results showed that degradation of *EP* involves a fast XRNA-dependent component and another one, slower and CAF1-dependent. However, a genome-wide transcriptome study, with XRNA knockdown mutants, showed that the main role of XRNA is in the degradation of unstable RNAs (8) and hence trypanosomes might degrade most RNAs by 3'->5' degradation pathway with the exosome. Nevertheless, further computational and experimental studies are needed.

VI.3. *Tb*CNOT10 is essential for the association of CAF1 with the NOT complex and its recruitment to mRNAs

*Tb*CNOT10 interacted directly with CAF1, NOT3/5 and with both the N- and C-terminal halves of NOT1 (Figure 16), which is similar to the interactions of CAF130 with NOT1 in yeast (83). Unlike *Tb*CNOT10, neither CAF130 nor human CNOT10 seem not to be essential for the integrity of the complex (77, this thesis). Although, I cannot exclude interactions via yeast NOT complex proteins, this idea seems rather unlikely since CNOT10 is absent in yeast. Surprisingly, it was seen that *Tb*CNOT10 and CAF1 interact with themselves, which is an indication that they might dimerize. This could be a further mechanism to regulate the activity of the complex, ensuring for instance that monomer CAF1 can only interact with the complex but not with dimerized CAF1.

Glycerol gradient analysis showed that about 50 % of V5-tagged CAF1 was not bound to the NOT complex. After CNOT10 depletion, the association of V5-tagged CAF1 to the complex was further diminished and, as mentioned above, mRNA turnover came to a halt. One can only speculate about the role of unbound CAF1, but one possibility is that it acts deadenylation-independently and represses translation as shown for Xenopus oocytes (174). Another possibility is that (unbound) CAF1 serves as a stock for newly formed NOT-complexes. Moreover, the depletion of *Tb*CNOT10 led to a reduction of

V5-*NOT1* protein level. Thus, *Tb*CNOT10 seems to be essential for the stable interaction of *CAF1* and *NOT1*, by interacting with each of them. The loss of CAF1 from the complex might lead to a structural change in NOT1, which could lead in turn to its degradation.

The reduction in deadenylation in *Tb*CNOT10-depleted cells led me to the assumption that *in vivo* free CAF1 by itself is unable to digest PABP-coated poly(A) tails. The easiest explanation for this observation is that CAF1 alone cannot be recruited to mRNAs. This is similar to *in vitro* experiments were the yeast CCR4-CAF1-NOT complex was not able to deadenylate PABP coated mRNAs (85). In contrast, once CAF1 is attached to mRNAs, either via the complex or by tethering, CAF1 is able to digest them. Similarly, in human cells depletion of NOT1 or NOT2 destabilised the CCR4-CAF1-NOT complex and decreased deadenylation activity in the cell (76, 79).

In our tandem affinity purification of *Tb*CNOT10, we did not identify RNA binding proteins that might be responsible for the recruitment of the complex to mRNAs. This is not surprising since the CAF1-NOT complex presumably interacts with many different proteins. Thus, RNA binding proteins might be underrepresented and/or interact only transiently with the NOT complex. A yeast two-hybrid screen with *Tb*CNOT10 as bait and a genomic library as prey could identify them. Moreover, *Tb*CNOT10 does not posses any known RNA binding domain, which would be necessary for a direct recruitment to mRNAs. Potential candidates for CAF1 recruitment might be CNOT3/5 and 9, which could pull-down several RNA binding proteins (e.g. TOB1, TOB2 and several zinc fingers) in HeLa cells (67).

VI.4. Function of CNOT10 is not conserved in evolution

In HEK cells, *Hs*CNOT10 is not needed for the stable association of *Hs*CAF1 with the NOT complex. Although *Hs*CNOT10 interacted with *Hs*CAF1a, its knockdown did not lead to a dissociation of *Hs*CAF1a from the complex, which was however achieved by a knockdown of *Hs*NOT1. This might be due to functionally redundant subunits, which compensate for the absence of *Hs*CNOT10. A major difference between human and trypanosomes, in this respect, is the gain of CCR4, TAB182 and C2ORF29 in

humans, which might stabilise the interaction of *Hs*CAF1 and NOT1 in the case of *Hs*CNOT10 depletion. Another possibility is that *Hs*CNOT10 is not needed for association of *Hs*CAF1 in the kidney, but in other tissues, since the expression pattern of subunits of the CCR4-CAF1-NOT complex is tissue-specific (69, 88). *Hs*CNOT10 might also help to target certain RNAs in the cell, but the role of *Hs*CNOT10 remains to be investigated.

VII. Current model and outlook

My results suggest that, in trypanosomes, *Tb*CNOT10 is important for the association of CAF1 with the NOT complex and its recruitment to mRNAs. It functions as follows: *Tb*CNOT10 is essential for the interaction of CAF1 with NOT1 and the integrity of NOT1. If *Tb*CNOT10 is depleted, CAF1 dissociates from the complex and loses its potential to bind mRNAs. Both the reduction of *Tb*CNOT10 and the dissociation of CAF1 lead to degradation of NOT1 (Figure 9).

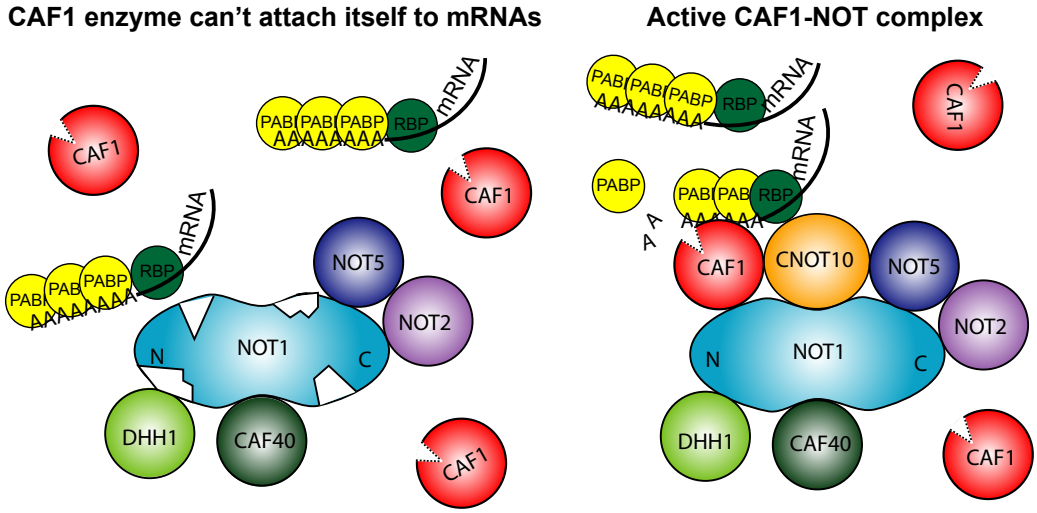

The role of *Tb*CNOT10 in the process of mRNA turnover

Left: In the absence of *Tb*CNOT10, CAF1 is not able to bind PABP-covered mRNAs and initiate mRNA degradation. Therefore, *Tb*CNOT10 is essential for CAF1's complex association and subsequent mRNA degradation. **Right**: Upon association with the complex, CAF1 is "tethered" to target mRNAs and some other subunits of the complex. Now it is able to degrade its target mRNA.

My study helped to broaden the understanding of mRNA turnover in *T. brucei*, but also triggered new questions. It is know that, in eukaryotic cells, the CCR4-CAF1-NOT complex can be recruited to mRNAs by RNA-binding proteins (74). In trypanosomes, no RNA-binding protein was identified to fulfil this role so far. The tandem affinity purification done for *Tb*CNOT10 did not reveal any RNA-binding proteins but a genome-wide yeast two-hybrid screen could find them. Thus, it would be interesting to include all other core subunits

of the complex (CAF1, NOT1, NOT2 and NOT3/5) in a genome-wide yeast-two hybrid screen in order to find all possible interaction partners of the complex. This would help to understand how the enzymatic activity of the major deadenylation complex is regulated. Another interesting experiment would be to tether *Tb*CNOT10 to a reporter mRNA in order to see if it is degraded. This would prove that *Tb*CNOT10 is able to recruit a functional CAF1-NOT complex. In the same line of thinking, it would also be interesting to see if *Tb*CNOT10 might bind directly to RNAs and hence might directly recruit the complex to its substrate. Although *Tb*CNOT10 does not contain any known RNA-binding domain, it was already shown that Pat1b could bind to RNAs without possessing any known domain (175, 176). To study the RNA-binding capacity of *Tb*CNOT10, recombinant protein need to be produced and tested with different RNA oligos in electrophoretic mobility shift assays (EMSA).

To study the role of *Hs*CNOT10, one should efficiently knock down *Hs*CNOT10 and analyse the degradation of a reporter mRNA. It would be interesting to see the impact of *Hs*CNOT10 depletion on deadenylation, steady-state levels and mRNA half-life. To identify if *Hs*CNOT10 is involved in RNA targeting, one should study its interaction partners by a yeast-two hybrid screen.

Finally as to better understand the interactions within the major deadenylation complex, it would be interesting to try to crystallise it.

VIII. Publication list

Faerber, V., Erben, E., Sharma, S., Stoecklin, G. Clayton, C. (Manuscript in preparation) In *T. brucei* CNOT10 is essential for the association of CAF1 to the CAF1-NOT complex and for its recruitment to mRNAs

Fadda, A.*, Faerber, V.*, Clayton C. (Manuscript in preparation) The role of CNOT10 and exoribonucleases in mRNA turnover

*shared first author

IX. Abbreviations

ARE	AU-rich element
Blast	Basic Local Alignment Search Tool
BS	Bloodstream
BSA	Bovine serum albumin
°C	degree celsius
CAF1	CCR4 associating factor 1
CCR4	Carbon catabolite repressor protein 4
CDS	Coding sequence
DNA	Deoxyribonucleic acid
DTT	Dithiothreitol
ECL	Enhanced chemical luminescence
GFP	Green fluorescence protein
HEK	Human embryonic kidney
HeLa	Henrietta Lacks
Hs	*Homo sapiens*
h	Hour
kb	Kilo base
kDa	Kilo Dalton
l	Liter
µ	Micro
m	Milli
min	Minute(s)
miRNA	Micro RNA
ml	Mililiter
mRNA	Messenger RNA
mRNP	Messenger ribonuleoprotein
n	Nano
NMD	Nonsense mediated decay
NOT	Negative on TATA
nt	Nucleotide
ORF	Open reading frame
PABP	Poly(A) tail binding protein
PAN	Pab1p-stimulated poly(A) ribonuclease
PARN	Poly(A)-ribonuclease
P-body	Processing body
PBS	Phosphate buffered saline
PC	Procyclic
PCR	Polymerase Chain Reaction
Puf	Pumilio/Fem-3-binding factor
RBP	RNA binding protein
re	Recombinant
RISC	RNA-induced silencing complex
RNA	Ribonucleic acid
RNAseq	RNA sequencing
RRM	RNA Recognition motif
RT	Room temperature
SDS-PAGE	Sodium dodecyl sulfate polyacrylamid gel
siRNA	Short interfering RNA

SL	Spliced leader
SRP	Signal recognition particle
SSC	Saline-sodium citrat
TAP	Tandem affinity purifcation
Tb	*Trypanosoma brucei*
TBS-T	Tris-Buffered Saline and Tween 20
TCA	Trichloroacetic acid
TPR	Tetratrico peptide repeat
TTP	Tristetraprolin
TRAMP	Trf4/5-Air1/2-Mtr4 polyadenylation complex
UTR	Untranslate region
V	Volt
VSG	Variant surface glycoprotein
XRN1	Exoribonuclease 1
XRNA	Exoribonuclease A

X. References

1. Staals, R.H. & Pruijn, G.J. The human exosome and disease. Adv Exp Med Biol 702, 132-142 (2010).
2. Audic, Y. & Hartley, R.S. Post-transcriptional regulation in cancer. Biol Cell 96, 479-498 (2004).
3. Sanduja, S., Blanco, F.F., Young, L.E., Kaza, V. & Dixon, D.A. The role of tristetraprolin in cancer and inflammation. Front Biosci 17, 174-188 (2012).
4. Srikantan, S. & Gorospe, M. HuR function in disease. Front Biosci 17, 189-205 (2012).
5. Carrick, D.M., Lai, W.S. & Blackshear, P.J. The tandem CCCH zinc finger protein tristetraprolin and its relevance to cytokine mRNA turnover and arthritis. Arthritis Res Ther 6, 248-264 (2004).
6. Steinacker, P., Aitken, A. & Otto, M. 14-3-3 proteins in neurodegeneration. Semin Cell Dev Biol 22, 696-704 (2011).
7. Bernstein, J.A., Khodursky, A.B., Lin, P.H., Lin-Chao, S. & Cohen, S.N. Global analysis of mRNA decay and abundance in Escherichia coli at single-gene resolution using two-color fluorescent DNA microarrays. Proc Natl Acad Sci U S A 99, 9697-9702 (2002).
8. Manful, T., Fadda, A. & Clayton, C. The role of the 5'-3' exoribonuclease XRNA in transcriptome-wide mRNA degradation. RNA 17, 2039-2047 (2011).
9. Wang, Y. *et al.* Precision and functional specificity in mRNA decay. Proc Natl Acad Sci U S A 99, 5860-5865 (2002).
10. Grigull, J., Mnaimneh, S., Pootoolal, J., Robinson, M.D. & Hughes, T.R. Genome-wide analysis of mRNA stability using transcription inhibitors and microarrays reveals posttranscriptional control of ribosome biogenesis factors. Mol Cell Biol 24, 5534-5547 (2004).
11. t Hoen, P.A. *et al.* mRNA degradation controls differentiation state-dependent differences in transcript and splice variant abundance. Nucleic Acids Res 39, 556-566 (2011).
12. Yang, E. *et al.* Decay rates of human mRNAs: correlation with functional characteristics and sequence attributes. Genome Res 13, 1863-1872 (2003).
13. Sharova, L.V. *et al.* Database for mRNA half-life of 19 977 genes obtained by DNA microarray analysis of pluripotent and differentiating mouse embryonic stem cells. DNA Res 16, 45-58 (2009).
14. Narsai, R. *et al.* Genome-wide analysis of mRNA decay rates and their determinants in Arabidopsis thaliana. Plant Cell 19, 3418-3436 (2007).
15. Goldstrohm, A.C. & Wickens, M. Multifunctional deadenylase complexes diversify mRNA control. Nat Rev Mol Cell Biol 9, 337-344 (2008).
16. Kahvejian, A., Roy, G. & Sonenberg, N. The mRNA closed-loop model: the function of PABP and PABP-interacting proteins in mRNA translation. Cold Spring Harb Symp Quant Biol 66, 293-300 (2001).
17. Amrani, N., Ghosh, S., Mangus, D.A. & Jacobson, A. Translation factors promote the formation of two states of the closed-loop mRNP. Nature 453, 1276-1280 (2008).

18. Sachs, A.B. & Varani, G. Eukaryotic translation initiation: there are (at least) two sides to every story. Nat Struct Biol 7, 356-361 (2000).
19. Schott, J. & Stoecklin, G. Networks controlling mRNA decay in the immune system. Wiley Interdiscip Rev RNA 1, 432-456 (2010).
20. Barreau, C., Paillard, L. & Osborne, H.B. AU-rich elements and associated factors: are there unifying principles? Nucleic Acids Res 33, 7138-7150 (2005).
21. Jiang, Y., Xu, X.S. & Russell, J.E. A nucleolin-binding 3' untranslated region element stabilizes beta-globin mRNA in vivo. Mol Cell Biol 26, 2419-2429 (2006).
22. Chen, C.Y. & Shyu, A.B. Mechanisms of deadenylation-dependent decay. Wiley Interdiscip Rev RNA 2, 167-183 (2011).
23. Shyu, A.B., Belasco, J.G. & Greenberg, M.E. Two distinct destabilizing elements in the c-fos message trigger deadenylation as a first step in rapid mRNA decay. Genes Dev 5, 221-231 (1991).
24. Yamashita, A. *et al.* Concerted action of poly(A) nucleases and decapping enzyme in mammalian mRNA turnover. Nat Struct Mol Biol 12, 1054-1063 (2005).
25. Brown, C.E. & Sachs, A.B. Poly(A) tail length control in Saccharomyces cerevisiae occurs by message-specific deadenylation. Mol Cell Biol 18, 6548-6559 (1998).
26. Tucker, M. *et al.* The transcription factor associated Ccr4 and CAF1 proteins are components of the major cytoplasmic mRNA deadenylase in Saccharomyces cerevisiae. Cell 104, 377-386 (2001).
27. Tharun, S. & Parker, R. Targeting an mRNA for decapping: displacement of translation factors and association of the Lsm1p-7p complex on deadenylated yeast mRNAs. Mol Cell 8, 1075-1083 (2001).
28. Wilusz, C.J., Gao, M., Jones, C.L., Wilusz, J. & Peltz, S.W. Poly(A)-binding proteins regulate both mRNA deadenylation and decapping in yeast cytoplasmic extracts. RNA 7, 1416-1424 (2001).
29. Mangus, D.A., Evans, M.C. & Jacobson, A. Poly(A)-binding proteins: multifunctional scaffolds for the post-transcriptional control of gene expression. Genome Biol 4, 223 (2003).
30. Muhlrad, D., Decker, C.J. & Parker, R. Deadenylation of the unstable mRNA encoded by the yeast MFA2 gene leads to decapping followed by 5'-->3' digestion of the transcript. Genes Dev 8, 855-866 (1994).
31. Coller, J. & Parker, R. Eukaryotic mRNA decapping. Annu Rev Biochem 73, 861-890 (2004).
32. Haas, G. *et al.* HPat provides a link between deadenylation and decapping in metazoa. J Cell Biol 189, 289-302 (2010).
33. Ozgur, S., Chekulaeva, M. & Stoecklin, G. Human Pat1b connects deadenylation with mRNA decapping and controls the assembly of processing bodies. Mol Cell Biol 30, 4308-4323 (2010).
34. Braun, J.E. *et al.* The C-terminal alpha-alpha superhelix of Pat is required for mRNA decapping in metazoa. EMBO J 29, 2368-2380 (2010).
35. Muhlrad, D. & Parker, R. Premature translational termination triggers mRNA decapping. Nature 370, 578-581 (1994).

36. Mullen, T.E. & Marzluff, W.F. Degradation of histone mRNA requires oligouridylation followed by decapping and simultaneous degradation of the mRNA both 5' to 3' and 3' to 5'. Genes Dev 22, 50-65 (2008).
37. Hu, W., Sweet, T.J., Chamnongpol, S., Baker, K.E. & Coller, J. Co-translational mRNA decay in Saccharomyces cerevisiae. Nature 461, 225-229 (2009).
38. Schwede, A. *et al.* A role for CAF1 in mRNA deadenylation and decay in trypanosomes and human cells. Nucleic Acids Res 36, 3374-3388 (2008).
39. Wiederhold, K. & Passmore, L.A. Cytoplasmic deadenylation: regulation of mRNA fate. Biochem Soc Trans 38, 1531-1536 (2010).
40. Berndt, H. *et al.* Maturation of mammalian H/ACA box snoRNAs: PAPD5-dependent adenylation and PARN-dependent trimming. RNA 18, 958-972 (2012).
41. Lin, W.J., Duffy, A. & Chen, C.Y. Localization of AU-rich element-containing mRNA in cytoplasmic granules containing exosome subunits. J Biol Chem 282, 19958-19968 (2007).
42. Chiba, Y. *et al.* AtPARN is an essential poly(A) ribonuclease in Arabidopsis. Gene 328, 95-102 (2004).
43. Wu, M. *et al.* Structural basis of m(7)GpppG binding to poly(A)-specific ribonuclease. Structure 17, 276-286 (2009).
44. Wu, M. *et al.* Structural insight into poly(A) binding and catalytic mechanism of human PARN. EMBO J 24, 4082-4093 (2005).
45. Gao, M., Fritz, D.T., Ford, L.P. & Wilusz, J. Interaction between a poly(A)-specific ribonuclease and the 5' cap influences mRNA deadenylation rates in vitro. Mol Cell 5, 479-488 (2000).
46. Dehlin, E., Wormington, M., Korner, C.G. & Wahle, E. Cap-dependent deadenylation of mRNA. EMBO J 19, 1079-1086 (2000).
47. Korner, C.G. & Wahle, E. Poly(A) tail shortening by a mammalian poly(A)-specific 3'-exoribonuclease. J Biol Chem 272, 10448-10456 (1997).
48. Korner, C.G. *et al.* The deadenylating nuclease (DAN) is involved in poly(A) tail removal during the meiotic maturation of Xenopus oocytes. EMBO J 17, 5427-5437 (1998).
49. Kang, M.K. & Han, S.J. Post-transcriptional and post-translational regulation during mouse oocyte maturation. BMB Rep 44, 147-157 (2011).
50. Kim, J.H. & Richter, J.D. Measuring CPEB-mediated cytoplasmic polyadenylation-deadenylation in Xenopus laevis oocytes and egg extracts. Methods Enzymol 448, 119-138 (2008).
51. Nishimura, N. *et al.* Analysis of ABA hypersensitive germination2 revealed the pivotal functions of PARN in stress response in Arabidopsis. Plant J 44, 972-984 (2005).
52. Nishimura, N. *et al.* ABA hypersensitive germination2-1 causes the activation of both abscisic acid and salicylic acid responses in Arabidopsis. Plant Cell Physiol 50, 2112-2122 (2009).
53. Lejeune, F., Li, X. & Maquat, L.E. Nonsense-mediated mRNA decay in mammalian cells involves decapping, deadenylating, and exonucleolytic activities. Mol Cell 12, 675-687 (2003).

54. Uchida, N., Hoshino, S. & Katada, T. Identification of a human cytoplasmic poly(A) nuclease complex stimulated by poly(A)-binding protein. J Biol Chem 279, 1383-1391 (2004).
55. Siddiqui, N. *et al.* Poly(A) nuclease interacts with the C-terminal domain of polyadenylate-binding protein domain from poly(A)-binding protein. J Biol Chem 282, 25067-25075 (2007).
56. Mangus, D.A. *et al.* Positive and negative regulation of poly(A) nuclease. Mol Cell Biol 24, 5521-5533 (2004).
57. Lowell, J.E., Rudner, D.Z. & Sachs, A.B. 3'-UTR-dependent deadenylation by the yeast poly(A) nuclease. Genes Dev 6, 2088-2099 (1992).
58. Schwede, A. *et al.* The role of deadenylation in the degradation of unstable mRNAs in trypanosomes. Nucleic Acids Res 37, 5511-5528 (2009).
59. Boeck, R. *et al.* The yeast Pan2 protein is required for poly(A)-binding protein-stimulated poly(A)-nuclease activity. J Biol Chem 271, 432-438 (1996).
60. Brown, C.E., Tarun, S.Z., Jr., Boeck, R. & Sachs, A.B. PAN3 encodes a subunit of the Pab1p-dependent poly(A) nuclease in Saccharomyces cerevisiae. Mol Cell Biol 16, 5744-5753 (1996).
61. Bonisch, C., Temme, C., Moritz, B. & Wahle, E. Degradation of hsp70 and other mRNAs in Drosophila via the 5' 3' pathway and its regulation by heat shock. J Biol Chem 282, 21818-21828 (2007).
62. Zheng, D. *et al.* Deadenylation is prerequisite for P-body formation and mRNA decay in mammalian cells. J Cell Biol 182, 89-101 (2008).
63. Braun, J.E., Huntzinger, E., Fauser, M. & Izaurralde, E. GW182 proteins directly recruit cytoplasmic deadenylase complexes to miRNA targets. Mol Cell 44, 120-133 (2011).
64. Collart, M.A. & Panasenko, O.O. The Ccr4-Not complex. Gene (2011).
65. Liu, H.Y. *et al.* The NOT proteins are part of the CCR4 transcriptional complex and affect gene expression both positively and negatively. EMBO J 17, 1096-1106 (1998).
66. Bai, Y. *et al.* The CCR4 and CAF1 proteins of the CCR4-NOT complex are physically and functionally separated from NOT2, NOT4, and NOT5. Mol Cell Biol 19, 6642-6651 (1999).
67. Lau, N.C. *et al.* Human Ccr4-Not complexes contain variable deadenylase subunits. Biochem J 422, 443-453 (2009).
68. Temme, C. *et al.* Subunits of the Drosophila CCR4-NOT complex and their roles in mRNA deadenylation. RNA 16, 1356-1370 (2010).
69. Albert, T.K. *et al.* Isolation and characterization of human orthologs of yeast CCR4-NOT complex subunits. Nucleic Acids Res 28, 809-817 (2000).
70. Temme, C., Zaessinger, S., Meyer, S., Simonelig, M. & Wahle, E. A complex containing the CCR4 and CAF1 proteins is involved in mRNA deadenylation in Drosophila. EMBO J 23, 2862-2871 (2004).
71. Viswanathan, P., Ohn, T., Chiang, Y.C., Chen, J. & Denis, C.L. Mouse CAF1 can function as a processive deadenylase/3'-5'-exonuclease in vitro but in yeast the deadenylase function of CAF1 is not required for mRNA poly(A) removal. J Biol Chem 279, 23988-23995 (2004).

72. Tucker, M., Staples, R.R., Valencia-Sanchez, M.A., Muhlrad, D. & Parker, R. Ccr4p is the catalytic subunit of a Ccr4p/Pop2p/Notp mRNA deadenylase complex in Saccharomyces cerevisiae. EMBO J 21, 1427-1436 (2002).
73. Dupressoir, A. *et al.* Identification of four families of yCCR4- and Mg2+-dependent endonuclease-related proteins in higher eukaryotes, and characterization of orthologs of yCCR4 with a conserved leucine-rich repeat essential for hCAF1/hPOP2 binding. BMC Genomics 2, 9 (2001).
74. Sandler, H., Kreth, J., Timmers, H.T. & Stoecklin, G. Not1 mediates recruitment of the deadenylase CAF1 to mRNAs targeted for degradation by tristetraprolin. Nucleic Acids Res 39, 4373-4386 (2011).
75. Fabian, M.R. *et al.* miRNA-mediated deadenylation is orchestrated by GW182 through two conserved motifs that interact with CCR4-NOT. Nat Struct Mol Biol 18, 1211-1217 (2011).
76. Ito, K., Takahashi, A., Morita, M., Suzuki, T. & Yamamoto, T. The role of the CNOT1 subunit of the CCR4-NOT complex in mRNA deadenylation and cell viability. Protein Cell 2, 755-763 (2011).
77. Azzouz, N. *et al.* Specific roles for the Ccr4-Not complex subunits in expression of the genome. RNA 15, 377-383 (2009).
78. Russell, P., Benson, J.D. & Denis, C.L. Characterization of mutations in NOT2 indicates that it plays an important role in maintaining the integrity of the CCR4-NOT complex. J Mol Biol 322, 27-39 (2002).
79. Ito, K. *et al.* CNOT2 depletion disrupts and inhibits the CCR4-NOT deadenylase complex and induces apoptotic cell death. Genes Cells 16, 368-379 (2011).
80. Albert, T.K. *et al.* Identification of a ubiquitin-protein ligase subunit within the CCR4-NOT transcription repressor complex. EMBO J 21, 355-364 (2002).
81. Dimitrova, L.N., Kuroha, K., Tatematsu, T. & Inada, T. Nascent peptide-dependent translation arrest leads to Not4p-mediated protein degradation by the proteasome. J Biol Chem 284, 10343-10352 (2009).
82. Garces, R.G., Gillon, W. & Pai, E.F. Atomic model of human Rcd-1 reveals an armadillo-like-repeat protein with in vitro nucleic acid binding properties. Protein Sci 16, 176-188 (2007).
83. Chen, J. *et al.* Purification and characterization of the 1.0 MDa CCR4-NOT complex identifies two novel components of the complex. J Mol Biol 314, 683-694 (2001).
84. Yao, G. *et al.* PAB1 self-association precludes its binding to poly(A), thereby accelerating CCR4 deadenylation in vivo. Mol Cell Biol 27, 6243-6253 (2007).
85. Simon, E. & Seraphin, B. A specific role for the C-terminal region of the Poly(A)-binding protein in mRNA decay. Nucleic Acids Res 35, 6017-6028 (2007).
86. Anderson, P. & Kedersha, N. RNA granules: post-transcriptional and epigenetic modulators of gene expression. Nat Rev Mol Cell Biol 10, 430-436 (2009).
87. Hoyle, N.P., Castelli, L.M., Campbell, S.G., Holmes, L.E. & Ashe, M.P. Stress-dependent relocalization of translationally primed mRNPs to

cytoplasmic granules that are kinetically and spatially distinct from P-bodies. J Cell Biol 179, 65-74 (2007).
88. Chen, C. *et al.* Distinct expression patterns of the subunits of the CCR4-NOT deadenylase complex during neural development. Biochem Biophys Res Commun 411, 360-364 (2011).
89. Fabian, M.R. *et al.* Mammalian miRNA RISC recruits CAF1 and PABP to affect PABP-dependent deadenylation. Mol Cell 35, 868-880 (2009).
90. Goldstrohm, A.C., Hook, B.A., Seay, D.J. & Wickens, M. PUF proteins bind Pop2p to regulate messenger RNAs. Nat Struct Mol Biol 13, 533-539 (2006).
91. Goldstrohm, A.C., Seay, D.J., Hook, B.A. & Wickens, M. PUF protein-mediated deadenylation is catalyzed by Ccr4p. J Biol Chem 282, 109-114 (2007).
92. Lee, D. *et al.* PUF3 acceleration of deadenylation in vivo can operate independently of CCR4 activity, possibly involving effects on the PAB1-mRNP structure. J Mol Biol 399, 562-575 (2010).
93. Kadyrova, L.Y., Habara, Y., Lee, T.H. & Wharton, R.P. Translational control of maternal Cyclin B mRNA by Nanos in the Drosophila germline. Development 134, 1519-1527 (2007).
94. Zaessinger, S., Busseau, I. & Simonelig, M. Oskar allows nanos mRNA translation in Drosophila embryos by preventing its deadenylation by Smaug/CCR4. Development 133, 4573-4583 (2006).
95. Semotok, J.L. *et al.* Smaug recruits the CCR4/POP2/NOT deadenylase complex to trigger maternal transcript localization in the early Drosophila embryo. Curr Biol 15, 284-294 (2005).
96. Jeske, M., Meyer, S., Temme, C., Freudenreich, D. & Wahle, E. Rapid ATP-dependent deadenylation of nanos mRNA in a cell-free system from Drosophila embryos. J Biol Chem 281, 25124-25133 (2006).
97. Chicoine, J. *et al.* Bicaudal-C recruits CCR4-NOT deadenylase to target mRNAs and regulates oogenesis, cytoskeletal organization, and its own expression. Dev Cell 13, 691-704 (2007).
98. Winkler, G.S. The mammalian anti-proliferative BTG/Tob protein family. J Cell Physiol 222, 66-72 (2010).
99. Ezzeddine, N. *et al.* Human TOB, an antiproliferative transcription factor, is a poly(A)-binding protein-dependent positive regulator of cytoplasmic mRNA deadenylation. Mol Cell Biol 27, 7791-7801 (2007).
100. Mauxion, F., Faux, C. & Seraphin, B. The BTG2 protein is a general activator of mRNA deadenylation. EMBO J 27, 1039-1048 (2008).
101. Jinek, M., Coyle, S.M. & Doudna, J.A. Coupled 5' nucleotide recognition and processivity in Xrn1-mediated mRNA decay. Mol Cell 41, 600-608 (2011).
102. Chang, J.H., Xiang, S., Xiang, K., Manley, J.L. & Tong, L. Structural and biochemical studies of the 5'-->3' exoribonuclease Xrn1. Nat Struct Mol Biol 18, 270-276 (2011).
103. Song, M.G. & Kiledjian, M. 3' Terminal oligo U-tract-mediated stimulation of decapping. RNA 13, 2356-2365 (2007).
104. Wu, L. & Belasco, J.G. Let me count the ways: mechanisms of gene regulation by miRNAs and siRNAs. Mol Cell 29, 1-7 (2008).

105. Huntzinger, E., Kashima, I., Fauser, M., Sauliere, J. & Izaurralde, E. SMG6 is the catalytic endonuclease that cleaves mRNAs containing nonsense codons in metazoan. RNA 14, 2609-2617 (2008).
106. Larimer, F.W. & Stevens, A. Disruption of the gene XRN1, coding for a 5'----3' exoribonuclease, restricts yeast cell growth. Gene 95, 85-90 (1990).
107. Larimer, F.W., Hsu, C.L., Maupin, M.K. & Stevens, A. Characterization of the XRN1 gene encoding a 5'-->3' exoribonuclease: sequence data and analysis of disparate protein and mRNA levels of gene-disrupted yeast cells. Gene 120, 51-57 (1992).
108. van Dijk, E.L. *et al.* XUTs are a class of Xrn1-sensitive antisense regulatory non-coding RNA in yeast. Nature 475, 114-117 (2011).
109. Lebreton, A., Tomecki, R., Dziembowski, A. & Seraphin, B. Endonucleolytic RNA cleavage by a eukaryotic exosome. Nature 456, 993-996 (2008).
110. Schneider, C., Leung, E., Brown, J. & Tollervey, D. The N-terminal PIN domain of the exosome subunit Rrp44 harbors endonuclease activity and tethers Rrp44 to the yeast core exosome. Nucleic Acids Res 37, 1127-1140 (2009).
111. Liu, Q., Greimann, J.C. & Lima, C.D. Reconstitution, activities, and structure of the eukaryotic RNA exosome. Cell 127, 1223-1237 (2006).
112. Assenholt, J. *et al.* Exonucleolysis is required for nuclear mRNA quality control in yeast THO mutants. RNA 14, 2305-2313 (2008).
113. Januszyk, K. & Lima, C.D. Structural components and architectures of RNA exosomes. Adv Exp Med Biol 702, 9-28 (2010).
114. Jia, H., Wang, X., Anderson, J.T. & Jankowsky, E. RNA unwinding by the Trf4/Air2/Mtr4 polyadenylation (TRAMP) complex. Proc Natl Acad Sci U S A 109, 7292-7297 (2012).
115. Tomecki, R., Drazkowska, K. & Dziembowski, A. Mechanisms of RNA degradation by the eukaryotic exosome. Chembiochem 11, 938-945 (2010).
116. Holub, P. *et al.* Air2p is critical for the assembly and RNA-binding of the TRAMP complex and the KOW domain of Mtr4p is crucial for exosome activation. Nucleic Acids Res 40, 5679-5693 (2012).
117. Buchon, N. & Vaury, C. RNAi: a defensive RNA-silencing against viruses and transposable elements. Heredity (Edinb) 96, 195-202 (2006).
118. Umbach, J.L. & Cullen, B.R. The role of RNAi and microRNAs in animal virus replication and antiviral immunity. Genes Dev 23, 1151-1164 (2009).
119. Valencia-Sanchez, M.A., Liu, J., Hannon, G.J. & Parker, R. Control of translation and mRNA degradation by miRNAs and siRNAs. Genes Dev 20, 515-524 (2006).
120. Okamura, K. Diversity of animal small RNA pathways and their biological utility. Wiley Interdiscip Rev RNA 3, 351-368 (2012).
121. Kulkarni, M., Ozgur, S. & Stoecklin, G. On track with P-bodies. Biochem Soc Trans 38, 242-251 (2010).
122. Cougot, N., Babajko, S. & Seraphin, B. Cytoplasmic foci are sites of mRNA decay in human cells. J Cell Biol 165, 31-40 (2004).

123. Andrei, M.A. *et al.* A role for eIF4E and eIF4E-transporter in targeting mRNPs to mammalian processing bodies. RNA 11, 717-727 (2005).
124. Brengues, M., Teixeira, D. & Parker, R. Movement of eukaryotic mRNAs between polysomes and cytoplasmic processing bodies. Science 310, 486-489 (2005).
125. Bhattacharyya, S.N., Habermacher, R., Martine, U., Closs, E.I. & Filipowicz, W. Stress-induced reversal of microRNA repression and mRNA P-body localization in human cells. Cold Spring Harb Symp Quant Biol 71, 513-521 (2006).
126. Erickson, S.L. & Lykke-Andersen, J. Cytoplasmic mRNP granules at a glance. J Cell Sci 124, 293-297 (2011).
127. Barrett, M.P., Vincent, I.M., Burchmore, R.J., Kazibwe, A.J. & Matovu, E. Drug resistance in human African trypanosomiasis. Future Microbiol 6, 1037-1047 (2011).
128. Brun, R., Blum, J., Chappuis, F. & Burri, C. Human African trypanosomiasis. Lancet 375, 148-159 (2010).
129. Queiroz, R., Benz, C., Fellenberg, K., Hoheisel, J.D. & Clayton, C. Transcriptome analysis of differentiating trypanosomes reveals the existence of multiple post-transcriptional regulons. BMC Genomics 10, 495 (2009).
130. Berriman, M. *et al.* The genome of the African trypanosome Trypanosoma brucei. Science 309, 416-422 (2005).
131. Liang, X.H., Haritan, A., Uliel, S. & Michaeli, S. trans and cis splicing in trypanosomatids: mechanism, factors, and regulation. Eukaryot Cell 2, 830-840 (2003).
132. Gilinger, G. & Bellofatto, V. Trypanosome spliced leader RNA genes contain the first identified RNA polymerase II gene promoter in these organisms. Nucleic Acids Res 29, 1556-1564 (2001).
133. Ben Amar, M.F. *et al.* The actin gene promoter of Trypanosoma brucei. Nucleic Acids Res 19, 5857-5862 (1991).
134. Lee, M.G. An RNA polymerase II promoter in the hsp70 locus of Trypanosoma brucei. Mol Cell Biol 16, 1220-1230 (1996).
135. Clayton, C.E. Life without transcriptional control? From fly to man and back again. EMBO J 21, 1881-1888 (2002).
136. Gunzl, A. *et al.* RNA polymerase I transcribes procyclin genes and variant surface glycoprotein gene expression sites in Trypanosoma brucei. Eukaryot Cell 2, 542-551 (2003).
137. Rudenko, G. Epigenetics and transcriptional control in African trypanosomes. Essays Biochem 48, 201-219 (2010).
138. De Gaudenzi, J., Frasch, A.C. & Clayton, C. RNA-binding domain proteins in Kinetoplastids: a comparative analysis. Eukaryot Cell 4, 2106-2114 (2005).
139. Wurst, M. *et al.* An RNAi screen of the RRM-domain proteins of Trypanosoma brucei. Mol Biochem Parasitol 163, 61-65 (2009).
140. Wurst, M. *et al.* Expression of the RNA recognition motif protein RBP10 promotes a bloodstream-form transcript pattern in Trypanosoma brucei. Mol Microbiol 83, 1048-1063 (2012).
141. Kramer, S. & Carrington, M. Trans-acting proteins regulating mRNA maturation, stability and translation in trypanosomatids. Trends Parasitol 27, 23-30 (2011).

142. Luu, V.D. *et al.* Functional analysis of Trypanosoma brucei PUF1. Mol Biochem Parasitol 150, 340-349 (2006).
143. Archer, S.K., Luu, V.D., de Queiroz, R.A., Brems, S. & Clayton, C. Trypanosoma brucei PUF9 regulates mRNAs for proteins involved in replicative processes over the cell cycle. PLoS Pathog 5, e1000565 (2009).
144. Droll, D. *et al.* The trypanosome Pumilio-domain protein PUF7 associates with a nuclear cyclophilin and is involved in ribosomal RNA maturation. FEBS Lett 584, 1156-1162 (2010).
145. Mani, J. *et al.* Alba-domain proteins of Trypanosoma brucei are cytoplasmic RNA-binding proteins that interact with the translation machinery. PLoS One 6, e22463 (2011).
146. Li, C.H. *et al.* Roles of a Trypanosoma brucei 5'->3' exoribonuclease homolog in mRNA degradation. RNA 12, 2171-2186 (2006).
147. Haile, S., Estevez, A.M. & Clayton, C. A role for the exosome in the in vivo degradation of unstable mRNAs. RNA 9, 1491-1501 (2003).
148. Utter, C.J., Garcia, S.A., Milone, J. & Bellofatto, V. PolyA-specific ribonuclease (PARN-1) function in stage-specific mRNA turnover in Trypanosoma brucei. Eukaryot Cell 10, 1230-1240 (2011).
149. Clayton, C. & Estevez, A. The exosomes of trypanosomes and other protists. Adv Exp Med Biol 702, 39-49 (2010).
150. Estevez, A.M., Kempf, T. & Clayton, C. The exosome of Trypanosoma brucei. EMBO J 20, 3831-3839 (2001).
151. Estevez, A.M., Lehner, B., Sanderson, C.M., Ruppert, T. & Clayton, C. The roles of intersubunit interactions in exosome stability. J Biol Chem 278, 34943-34951 (2003).
152. Haile, S., Cristodero, M., Clayton, C. & Estevez, A.M. The subcellular localisation of trypanosome RRP6 and its association with the exosome. Mol Biochem Parasitol 151, 52-58 (2007).
153. Cristodero, M. & Clayton, C.E. Trypanosome MTR4 is involved in rRNA processing. Nucleic Acids Res 35, 7023-7030 (2007).
154. Delhi, P., Queiroz, R., Inchaustegui, D., Carrington, M. & Clayton, C. Is there a classical nonsense-mediated decay pathway in trypanosomes? PLoS One 6, e25112 (2011).
155. Cassola, A., De Gaudenzi, J.G. & Frasch, A.C. Recruitment of mRNAs to cytoplasmic ribonucleoprotein granules in trypanosomes. Mol Microbiol 65, 655-670 (2007).
156. Holetz, F.B. *et al.* Evidence of P-body-like structures in Trypanosoma cruzi. Biochem Biophys Res Commun 356, 1062-1067 (2007).
157. Kramer, S. *et al.* Heat shock causes a decrease in polysomes and the appearance of stress granules in trypanosomes independently of eIF2(alpha) phosphorylation at Thr169. J Cell Sci 121, 3002-3014 (2008).
158. Altschul, S.F. *et al.* Gapped BLAST and PSI-BLAST: a new generation of protein database search programs. Nucleic Acids Res 25, 3389-3402 (1997).
159. Gough, J., Karplus, K., Hughey, R. & Chothia, C. Assignment of homology to genome sequences using a library of hidden Markov models that represent all proteins of known structure. J Mol Biol 313, 903-919 (2001).

160. Clayton, C.E. *et al.* Down-regulating gene expression by RNA interference in Trypanosoma brucei. Methods Mol Biol 309, 39-60 (2005).
161. Alsford, S. *et al.* High-throughput phenotyping using parallel sequencing of RNA interference targets in the African trypanosome. Genome Res 21, 915-924 (2011).
162. Gavin, A.C. *et al.* Functional organization of the yeast proteome by systematic analysis of protein complexes. Nature 415, 141-147 (2002).
163. Maillet, L., Tu, C., Hong, Y.K., Shuster, E.O. & Collart, M.A. The essential function of Not1 lies within the Ccr4-Not complex. J Mol Biol 303, 131-143 (2000).
164. D'Andrea, L.D. & Regan, L. TPR proteins: the versatile helix. Trends Biochem Sci 28, 655-662 (2003).
165. Golovanov, A.P., Hautbergue, G.M., Wilson, S.A. & Lian, L.Y. A simple method for improving protein solubility and long-term stability. J Am Chem Soc 126, 8933-8939 (2004).
166. Shalem, O., Groisman, B., Choder, M., Dahan, O. & Pilpel, Y. Transcriptome kinetics is governed by a genome-wide coupling of mRNA production and degradation: a role for RNA Pol II. PLoS Genet 7, e1002273 (2011).
167. Lotan, R. *et al.* The RNA polymerase II subunit Rpb4p mediates decay of a specific class of mRNAs. Genes Dev 19, 3004-3016 (2005).
168. Lotan, R., Goler-Baron, V., Duek, L., Haimovich, G. & Choder, M. The Rpb7p subunit of yeast RNA polymerase II plays roles in the two major cytoplasmic mRNA decay mechanisms. J Cell Biol 178, 1133-1143 (2007).
169. Navarro, M., Penate, X., Landeira, D. & Lopez-Farfan, D. Role of RPB7 in RNA pol I transcription in Trypanosoma brucei. Mol Biochem Parasitol 180, 43-44 (2011).
170. Gunzl, A., Park, S.H., Nguyen, T.N., Kirkham, J.K. & Lee, J.H. Response to "Role of RPB7 in RNA pol I transcription in Trypanosoma brucei". Mol Biochem Parasitol 180, 45-46 (2011).
171. Park, S.H., Nguyen, T.N., Kirkham, J.K., Lee, J.H. & Gunzl, A. Transcription by the multifunctional RNA polymerase I in Trypanosoma brucei functions independently of RPB7. Mol Biochem Parasitol 180, 35-42 (2011).
172. Penate, X. *et al.* RNA pol II subunit RPB7 is required for RNA pol I-mediated transcription in Trypanosoma brucei. EMBO Rep 10, 252-257 (2009).
173. Devaux, S. *et al.* Characterization of RNA polymerase II subunits of Trypanosoma brucei. Mol Biochem Parasitol 148, 60-68 (2006).
174. Cooke, A., Prigge, A. & Wickens, M. Translational repression by deadenylases. J Biol Chem 285, 28506-28513 (2010).
175. Pilkington, G.R. & Parker, R. Pat1 contains distinct functional domains that promote P-body assembly and activation of decapping. Mol Cell Biol 28, 1298-1312 (2008).
176. Totaro, A. *et al.* The human Pat1b protein: a novel mRNA deadenylation factor identified by a new immunoprecipitation technique. Nucleic Acids Res 39, 635-647 (2011).